FINNISH METEOROLOGICAL INSTITUTE CONTRIBUTIONS No. 149

Seasonal snow surface roughness and albedo

Kati Anttila

Faculty of Science

Geophysics

University of Helsinki

Helsinki, Finland

Academic dissertation

To be presented, with the permission of the Faculty of Science of the University of Helsinki, for public criticism in E204 auditorium at Physicum (Gustaf Hällströmin katu 2 A, Helsinki) on April 26th, 2019, at 12 o'clock noon.

Helsinki, 2019

Supervisors Dr. Terhikki Manninen
Meteorological Research, Satellite and Radar Applications
Finnish Meteorological Institute

Research Professor Sanna Kaasalainen
Navigation and Positioning, Sensors and Indoor Navigation
Finnish Geospatial Research Institute of the National Land survey of Finland

Professor (emeritus) Matti Leppäranta
Institute for Atmospheric and Earth System Research/ Physics
University of Helsinki

Pre-examiners
Dr. Lasse Makkonen
VTT Technical Research Centre of Finland

Dr. Ghislain Picard
Institue des Géosciences de l'Environnement
Université Grenoble Alpes, France

Custos Professor Petteri Uotila
Institute for Atmospheric and Earth System Research/ Physics
University of Helsinki

Opponent Professor Richard Essery
School of Geosciences
University of Edinburg

ISBN: 978-952-336-063-1 (paperback)
ISBN: 978-952-336-064-8 (pdf)
ISSN: 0782-6117

ILMATIETEEN LAITOS

Julkaisija
Ilmatieteen laitos, (Erik Palménin aukio 1)
PL 503, 00101 Helsinki

Julkaisun sarja, numero ja raporttikoodi
Finnish Meteorological Institute Contributions 149,
FMI-CONT-149
Julkaisuaika Huhtikuu 2019

Tekijä Kati Anttila

Nimeke
Kausittaisen lumipeitteen pinnan karkeus ja albedo

Tiivistelmä

Tämä väitöskirja käsittelee kausittaisen lumipeitteen pinnan karkeutta ja kirkkautta hyödyntäen optista satelliittiaineistoa ja laserkeilausta. Maan pinnan kaukokartoitus tarvitsee tietoa maan pinnan säteilyominaisuuksista. Lumipinnat heijastavat suurimman osan auringosta tulevasta säteilystä takaisin ilmakehään ja avaruuteen. Kausittainen lumipeite kattaa laajan alueen pohjoisen pallonpuoliskon maa-alasta. Alueellisen kattavuutensa ja kirkkautensa vuoksi sillä on merkittävä vaikutus maapallon energiataseeseen ja siten ilmastoon. Lumipinnan heijastusominaisuudet, kuten esimerkiksi pinnan karkeus, vaikuttavat suoraan lumipinnan kirkkauteen. Tässä väitöskirjassa on tarkasteltu kahta lumen pinnan karkeuden mittausmenetelmää. Ensimmäinen näistä tekniikoista perustuu lumeen asetetun mustan levyn valokuvaamiseen. Levystä ja lumipinnasta otetusta kuvasta etsitään automaattisesti lumipinnan profiili. Tämä tekniikka on helppokäyttöinen ja luotettava myös kenttäolosuhteissa. Sillä saadaan kerättyä tietoa lumen pinnan karkeudesta alle millimetrin tarkkuudella. Toisessa mittausmenetelmässä laserkeilainta liikutetaan moottorikelkalla. Näin saadaan katettua laaja alue, josta syntyy 3D havaintoja.

Pinnan karkeutta kuvaavien suureiden arvoihin vaikuttaa analysoidun profiilin pituus tai alueen laajuus. Kaukokartoituksen kannalta on oleellista mitata pinnankarkeutta kaikissa sovellukselle oleellisissa mittakaavoissa. Maan pinnan sirontamallit käyttävät pinnan karkeuden kuvaamiseen vain yhtä suuretta. Siten tämän suureen tulisi sisältää tietoa useista mittakaavoista. Tässä väitöskirjassa kerättiin Sodankylän alueelta 669 lumiprofiilia levymenetelmää käyttäen. Nämä profiilit analysoitiin käyttäen suureita, jotka kuvaavat profiilin korkeusvaihtelun riippuvuutta mitatusta matkasta ja sisältävät siten tietoa useista mittakaavoista. Käyttämällä näitä suureita kyettiin erottelemaan eri lumipintoja niiden iän ja lumityypin mukaan.

Satelliittien instrumentit mittaavat kerralla laajoja alueita. Maan pinnalla tehtävillä pistemäisiä alueita kuvaavilla havainnoilla selvitetään, kuinka laadukkaita satelliittituotteet, kuten lumi- ja albedotuotteet, ovat. Koska pintahavaintojen ja satelliittihavaintojen kattamat alueet eivät ole samat, itse ahavainnotkaan eivät täysin vastaa toisiaan. Laserkeilausaineistot kattavat laajempia alueita kuin perinteisin menetelmin tuotetut havainnot ja ovat siten lupaavia satelliittiaineistojen arviointiin. Tämän väitöskirjan sisältämä tutkimus lasersäteen käyttäytymisestä lumipinnoilla edistää laserkeilausaineistojen käytettävyyttä lumeen liittyvässä tutkimuksessa ja satelliittiaineistojen laadun määrittämisessä. Tulosten mukaan kuivasta lumesta lasersäde heijastuu takaisin aivan lumen pinnasta, kun taas märässä lumessa se heijastuu noin 1 cm syvyydestä. Takaisin heijastuneen lasersäteen kirkkaus riippuu tulokulmasta samalla tavalla erityyppisillä lumipinnoilla. Siten tulokulman vaikutus laserhavainnon kirkkauteen voidaan korjata samalla tavalla kaikilla mitatuilla lumipinnoilla.

Tämän väitöskirjan viimeisessä osassa tutkittiin kausittaisen lumipeitteen peittämien alueiden pinnan kirkkauden (albedon) ja sulamiskauden ajankohdan muutoksia vuosina 1982-2015 pohjoisen pallon puoliskon maa-alueilla leveyspiirien 40°N ja 80°N välillä. Tutkimus keskittyi sulamiskautta edeltävään pinnan kirkkauteen, joka oli muuttunut huomattavasti boreaalisen metsävyöhykkeen alueella. Muutos oli erisuuntaista eri alueilla. Tundralla sulamista edeltävä pinnan kirkkaus ei ollut muuttunut. Sulamiskausi oli aikaistunut Keski-Siperian ylängöllä ja pidentynyt Kiinan, Mongolian ja Venäjän rajaa ympäröivällä alueella sekä Kanadan Kalliovuorten pohjois-osissa. Pinnan kirkkauden muutokset olivat sidoksissa kasvillisuuden muutoksiin, kun taas sulamiskauden ajankohdan muutoksiin vaikuttivat enemmän ilmastolliset tekijät.

Tämä väitöskirja parantaa kausittaisen lumipeitteen pinnan sirontaominaisuuksien ymmärtämistä ja sen tuloksia voidaan käyttää kaukokartoitusaineistojen ja ilmastomallien kehittämisessä.

Julkaisijayksikkö Ilmatieteen laitos		
Luokitus (UDK) 551.32, 528.8, 550.3	Asiasanat lumi, albedo, kaukokartoitus, laserkeilaus	
ISSN ja avainnimike 0782-6117 Finnish Meteorological Institute Contributions		
ISBN 978-952-336-063-1 (nid.) 978-952-336-064-8 (pdf)	Kieli englanti	Sivumäärä 162

FINNISH METEOROLOGICAL INSTITUTE

Published by	Finnish Meteorological Institute (Erik Palménin aukio 1), P.O. Box 503 FIN-00101 Helsinki, Finland	Series title, number and report code of publication Finnish Meteorological Institute Contributions 149, FMI-CONT-149 Date April 2019

Author Kati Anttila

Title Seasonal snow surface roughness and albedo

Abstract

The topic of this dissertation is the seasonal snow surface roughness and albedo. These are studied using optical satellite data and terrestrial laser scanning.

The use of remote sensing data requires knowledge on the optical properties of the measured surface. For snow, these properties are affected by surface roughness. In this dissertation, two different methods for measuring snow surface roughness were validated and used in the field. One of them is based on plate photography. It is easy to use in the field and able to study surface features in sub-millimeter scale. The other method is based on mobile laser scanning and is able to produce 3D surface descriptions of large areas. The plate-photography-based method was used in the field to gather 669 profiles of the snow surface. The profiles were analyzed using multiscale parameters.

The validation of satellite data requires observations at the surface. This validation data typically consists of pointwise measurements, whereas the satellite data observations cover larger areas. Laser scanning provides data that cover larger areas, thus more in line with the satellite data. This could in the future be used for satellite data validation. The usability of laser scanning data on snow surfaces was improved by studying the incidence angle dependency of the laser scanning intensity data on different snow types. A function for correcting the incidence angle effect on all measured snow types was developed. The backscattering of laser beam on snow surface was found to take place at the very surface for dry snow, and within 1cm depth for wet snow.

The final part of this dissertation studies the changes in surface albedo prior to melting and the timing of the melt season in Northern Hemisphere land areas between 40°N and 80°N. The albedo prior to melt had changed significantly in the boreal forest area, but not in the tundra. The direction of change is different in different areas. The melt season takes place at the same time of year for most of the study area, but for Central Siberian Plane the melt season takes place earlier. In Northern Canadian Rocky Mountains and in the area around the borders of Russia, China and Mongolia the melt starts earlier and ends later, thus resulting in longer melt seasons. The changes observed in the pre-melt albedo are related to vegetation, whereas the melt season timing is more related to the climatic parameters.

The results of this dissertation can be used in developing remote sensing data and climate models through improved understanding of seasonal snow surface roughness and albedo.

Publishing unit Finnish Meteorological Institute

Classification (UDC) 551.32, 528.8, 550.3 Keywords: snow, albedo, laser scanning, remote sensing

ISSN and series title
0782-6117 Finnish Meteorological Institute Contributions

ISBN	Language	Pages
978-952-336-063-1 (nid.) 978-952-336-064-8 (pdf)	English	162

PREFACE

The work presented in this dissertation was carried out both at the former Finnish Geodetic Institute and The Finnish Meteorological Institute in 2009-2018. During these years I have come to learn that being a scientist is not about what you know, it's what the people around you know. It is never possible to know everything you need, so having people around you whose skills complement yours is essentially important. I have been surrounded by skillful and kind people whose support and expertise has been invaluable.

First and foremost I would like to express my deepest gratitude to my advisors, Dr. Terhikki Manninen and Professor Sanna Kaasalainen. Besides all the skill you need while being a scientist, you have taught me integrity and persistence. You have shown me how to survive in the world of science as it is today and supported me on the rocky parts of the path. Your passion and commitment is truly inspiring.

I also wish to thank my supervisor from the university, Professor (emeritus) Matti Leppäranta and the custos for this defense, Professor Petteri Uotila. You have served as a link to the university and have guided me through the jungle of the changing university protocol.

I thank Professor Essery for agreeing to be the opponent for this dissertation, and Dr. Ghislain Picard and Dr. Lasse Makkonen for their constructive comments as pre-examiners. These comments have improved the readability and content of is introduction.

Most of the daily work is done with the group members and co-authors of the papers included in this dissertation: Terhikki, Sanna, Panu, Aku, Niilo, Emmihenna, Antero, Harri, Teemu, Olli, Anssi, Anttoni, Elena, Viivi, Kerttu, Ljuba, Vesa, Aulikki, Tuure. Your effort and support on the stormy seas of publishing and project work is truly appreciated. Your work made this dissertation possible.

I also wish to thank my colleagues at FMI and FGI, with whom I have had so many inspiring and supportive conversations over the years on all aspects of life. You have offered me support when times have been rough and helped me organize my thoughts when I have lost the direction and big picture. You have helped me laugh at the obscurities and unfairness. The work of a scientist today is project work in international teams. I wish to thank my colleagues in the CM SAF and H SAF projects teams, DWD, SMHI, KNMI, MeteoSwiss, RMI, UKMO, SYKE, MeteoFrance and CNRS.

Besides being a job, the doctoral studies are a process of personal growth. I wish to thank my friends and relatives for the invaluable support you have given me. You have helped me forget work from time to time and reminded me of the real life. You have helped me put things in perspective and reminded me of the importance of laughter.

Finally, I would like to thank my parents and sister for their never-ending faith in me, also in times when my own faith has been missing. I thank you for your patience and support and your efforts to create circumstances that enable me to concentrate on the work at hand. Without you I would never have gotten to where I am now. You remind me by existing, that with or without PhD, life will continue. Now at the final parts of this project I feel that this whole path is a proof on what you have taught me: things do tend to work out.

Helsinki, 13th November 2018

Kati Anttila

CONTENTS

LIST OF PUBLICATIONS AND AUTHOR'S CONTRIBUTION

This dissertation contains an introductory review, followed by five research papers. In the introductory part, the articles are referred to by their roman numerals.

I Manninen, T., Anttila, K., Karjalainen, T., & Lahtinen, P. (2012). Automatic snow surface roughness estimation using digital photos. *Journal of Glaciology*, *58*(211), 993-1007.

In paper I Anttila took part in planning the calibration measurements, made the measurements, and participated in the analysis of the calibration measurements and writing the paper.

II Anttila, K., Manninen, T., Karjalainen, T., Lahtinen, P., Riihelä, A., & Siljamo, N. (2014). The temporal and spatial variability in submeter scale surface roughness of seasonal snow in Sodankylä Finnish Lapland in 2009–2010. *Journal of Geophysical Research: Atmospheres*, *119*(15), 9236-9252.

In paper II Anttila took part in the field measurements, having conducted most of the 2010 plate measurements and some of the snow pit measurements. She analyzed the extracted profiles and snow pit data and wrote most of the paper.

III Kukko, A., Anttila, K., Manninen, T., Kaasalainen, S., & Kaartinen, H. (2013). Snow surface roughness from mobile laser scanning data. *Cold Regions Science and Technology*, *96*, 23-35.

In paper III Anttila made the plate measurements and the data analysis on the plate and laser scanning profiles. She also wrote the paper together with the first author A. Kukko.

IV Anttila, K., Hakala, T., Kaasalainen, S., Kaartinen, H., Nevalainen, O., Krooks, A., ... & Jaakkola, A. (2016). Calibrating laser scanner data from snow surfaces: Correction of intensity effects. *Cold Regions Science and Technology*, *121*, 52-59.

In paper IV Anttila planned and conducted the measurements with help from the other authors. She also analyzed the results and wrote most of the paper.

V Anttila, K., Manninen, T., Jaaskelainen, E., Riihela, A., & Lahtinen, P. (2018). The Role of Climate and Land Use in the Changes in Surface Albedo Prior to Snow Melt and the Timing of Melt Season of Seasonal Snow in Northern Land Areas of 40°N–80°N during 1982–2015. *Remote Sensing, 10(*10*),* 1619, https://doi.org/10.3390/rs10101619

In paper V Anttila analyzed the extracted melt season parameters and wrote most of the paper.

ABBREVIATIONS

ALS	Airborne Laser Scanning
BRDF	Bidirectional Reflectance Distribution Function
CLARA-A2 SAL	Satellite Application Facility for Climate Monitoring (CM SAF, funded by EUMETSAT) CLouds, Albedo and RAdiation second release Surface ALbedo (CLARA-A2 SAL) data record
CM SAF	Satellite Application Facility for Climate Monitoring
ECMWF	The European Centre for Medium-Range Weather Forecasts
ECV	Essential climate variable
ERA-Interim	Reanalysis data record by ECMWF
EUMETSAT	the European Organisation for the Exploitation of Meteorological Satellites
FGI	Finnish Geodetic Institute
FGI ROAMER	Road Environment Mapping System of the Finnish Geodetic Institute
FMI	Finnish Meteorological Institute
FMI-ARC	The Arctic Research Center of the Finnish Meteorological Institute
GCOS	Global Climate Observing System
HSL	Hyperspectral Laser Scanning
IMU	Inertial Measurement Unit
IPCC	Intergovernmental Panel on Climate Change
MLS	Mobile Laser Scanning
NDVI	Normalized Difference Vegetation Index
TLS	Terrestrial Laser Scanning
rms	root mean square
SAL	Surface albedo
SCE	Snow Cover Extent
SNORTEX	Snow Reflectance Transition Experiment
SSA	Specific Surface Area
SWE	Snow Water Equivalent
UNFCCC	United Nations Framework Convention on Climate Change

SYMBOLS

α_{ia}	Incidence angle
α_{bsa}	Black sky surface albedo
θ_t	Transmitter beam width
Θ_v	Zenith angle of reflected solar radiation
Θ_s	Zenith angle of the incident solar radiation
P	reflectance
σ_h	root mean square height variation
σ_b	Backscatter cross section
ϕ_v	Azimuth angle of the reflected solar radiation
ϕ_s	Azimuth angle of the incident solar radiation
D_r	Receiver aperture
P_r	Power received by radar
P_t	Transmitter power
R^2	Coefficient of determination
R_l	Range of radar measurement

1. INTRODUCTION

Seasonal snow cover can occupy 50% of the land area of the Northern Hemisphere (Mialon et al. 2005). This affects both the lives of people living in the area by putting strains on the infrastructure (Makkonen 1989) and the environment. The large spatial coverage together with the high reflectivity of snow makes it an important factor for the global energy budget (Flanner et al. 2011). The reflective properties of the snow surface are directly dependent on the geophysical properties of the snow. Given the high variability of snow geophysical properties around the globe, also the behavior of light on the snow surface varies between different areas. Understanding climate requires understanding the reflective properties, such as surface albedo, of snow, and thus the geophysical processes and characteristics, such as surface roughness, of the snow. This is the motivation behind the work presented in this dissertation.

One of the geophysical properties affecting the reflectance of the snow surface is snow surface roughness. The measurements of snow surface roughness are relatively few and they are made in different scales and resolutions. Most of the existing studies on snow surface roughness describe the large scale roughness (Leroux & Fily 1998, Warren et al. 1998, van der Veen et al. 2009, Kuchiki et al. 2011, Zhuravleva & Kokhanovsky 2011, Picard et al. 2016). The work on small scale roughness is still very limited, possibly due to the lack of methods available. Also the present day surface albedo models include information on the large scale surface roughness, but small scale surface roughness is still missing. The work on small scale roughness is starting fast, with new methods being developed and parameters being tested. This dissertation contributes to developing methods to study small and medium scale surface roughness by presenting two new methods to measure the snow surface structures.

Small-scale roughness can be measured using a background plate that is partially inserted into the snow. The interface between the plate and the snow surface forms a profile of the snow surface, which is then used to describe the surface features. Different methods have different ways of extracting the profile, which are in different scales, resolutions and level of accuracy. Large-scale roughness is often measured using laser scanning, typically airborne laser scanning having relatively low resolution.

The parameters used to describe snow surface roughness are many. The applications related to the optical properties of the snow surface use root mean square height variation, correlation length, and autocorrelation functions, which are also the parameters used in scattering models. Since the snow surface roughness (being the height variation) depends on the measured scale and resolution, the parameters used should be

able to describe the surface at all relevant scales. This dissertation studies the use of multiscale parameters in describing the snow surface height variation.

In climate studies, the brightness of the surface is described as surface albedo. It is an essential climate variable (ECV) defined in the Implementation Plan for Global Observing System for Climate in support of the United Nations Framework Convention on Climate Change (GCOS Secretariat 2006). The relationship between large scale surface roughness and albedo has been studied previously (Leroux & Fily 1998, Warren et al. 1998, Kuchiki et al. 2011, Zhuravleva & Kokhanovsky 2011), but the effect of small scale surface roughness on surface albedo is still largely unknown. The existing studies show both a darkening of surface albedo (Leroux & Fily 1998, Warren et al. 1998, Kuchiki et al. 2011, Zhuravleva & Kokhanovsky 2011) and a change in small scale surface roughness as the snow ages (paper II), suggesting a link between surface albedo and surface roughness. However, further studies are needed to know the relationship in more detail.

The importance of surface albedo on the global and local climate requires the understanding of the behavior of albedo at a global scale. In practice, this means using satellite data and products. Recently the advancements in satellite data processing and availability have enabled the processing of surface albedo data records that are long enough for climate studies. Paper IV utilizes one of these data records (CLARA-A2 SAL) to study the changes in surface albedo prior to melt and melt season timing of areas covered with seasonal snow.

The satellite-based albedo and snow products need to be validated against in situ measurements. Most of these are pointwise measurements or cover only a small area. Since the satellite data comes in resolutions of tens of meters to kilometers, there is a clear gap between the scales of the satellite and validation data. In addition to this, the in situ measurements typically cover only one type of surface, whereas the reflectance observed by the satellite instrument comes from a mixture of different land cover types and the atmosphere. Therefore the in situ measurements do not fully represent the areas covered by the footprints of the satellite observations. This is especially the case in areas with fractured land use features, such as in the boreal forest zone, where the land surface features vary in small scales.

In order to be able to validate satellite-derived albedo and snow products, the validation data would need to cover larger areas. Laser scanning offers a means to cover larger areas, thus providing a better representativeness for the satellite data validation (Kenner et al. 2011, Egli et al. 2012, paper III, Picard et al. 2016). So far the use of laser scanning data for satellite data validation is not common and methods are still being developed. More information is still needed on the behavior of laser scanning range and intensity data on snow surfaces. Once the open issues about the data have been solved, laser scanning can be used in several glaciological applications. This dissertation provides information on the backscattering of laser beam from different types of snow surfaces, thus enhancing the usability of laser scanning on measuring snow surfaces.

The improved satellite-based albedo and snow products give means to study the changes in these on a global scale. Recently, global satellite-derived time series on snow and albedo of several decades have provided information on the long-term changes in the snow cover. The studies on the time series data reveal changes in the snow cover extent, melt season timing and albedo during the spring months of northern hemisphere (Derý & Brown 2007, Markus 2009, Brown & Robinson 2011, Derksen & Brown 2012, Wang et al. 2013, Atlaskina et al. 2015, Chen et al. 2015, Malnes et al. 2016).

The main objective of this dissertation is to study the seasonal snow surface roughness and albedo using optical satellite data and laser scanning. This includes developing methods to measure snow surface roughness and studying the usability of laser scanning on snow surface, which could potentially be used for satellite data validation and snow surface scattering modelling. The work presented here provides the basis for future work on studying the role of small scale surface roughness on seasonal snow surface albedo.

The specific objectives of this dissertation are:

- To develop methods for measuring small scale seasonal snow surface roughness (papers I, II, III)
- To study the usability of multiscale parameters to describe the snow surface roughness (paper II)
- To study the behavior of small scale surface roughness of seasonal snow in boreal forest zone (paper II)
- To develop methods and improve the usability of laser scanning on snow-covered surfaces (papers III and IV)
- To study the changes in large scale surface albedo of snow-covered surfaces (paper V)

2. LIGHT TRANSFER, OPTICAL PROPERTIES AND ALBEDO OF SNOW

The optical properties of snow depend on the type of snow crystals, surface roughness and amount of liquid water at and near the surface of the snowpack. The scattering properties are most heavily determined by particle size and shape (Shi & Dozier 2000). Also surface roughness depends on the type of snow crystals and their arrangement on the surface.

The characteristics of the snow surface are first affected by the falling snowflakes, which can take several different forms (Nakaya 1954, Magono & Lee 1966, Libbrecht 2005, Lamb & Verlinde 2011). As the snowflakes reach the ground, the cohesion between snow crystals makes the crystals attach to the surface at first contact instead on being arranged to a position of minimum energy (Löwe et al. 2007). The arrangement of the crystals also depends on the prevailing wind conditions. After the snowflakes have fallen on the ground they start to reshape. These metamorphic processes can be divided into mechanic, dry and wet metamorphism (Sommerfield & LaChapelle 1970). Mechanic metamorphism is typical in cold temperatures, where the absence of liquid water give the wind possibility to redistribute and mechanically round the crystals. During transportation by air, the surface snow particles change shape by breaking into smaller particles and gaining mass from moisture in the surrounding air both through accretion and aggregation (Armstrong & Brun 2008). New snow falling on top of the crystals also causes mechanical breaking of the crystals.

If the snowpack is dry, that is, there is no liquid water, the ice sublimates from the snow crystals and possibly gathers on other crystals. This causes angular crystals to become rounded crystals as the water vapor is sublimated from the convex surfaces and gathered in the concave parts (Colbeck 1982a). In addition to rounding of the crystals by sublimation, sintering forms ice bonds between different grains resulting in larger grains (Colbeck 1997) and kinetic growth metamorphism causes the rounded crystals to grow into faceted crystals (Colbeck 1982b). In wet snow, there is liquid water within the snowpack. The melting and refreezing of water reshape the grains and forms layers of different density and grain structure in the snowpack (Figure 1).

At the snow surface, solar radiation can either be reflected back to the atmosphere or absorbed into the snowpack. At the visible wavelengths, absorption is much weaker than reflectance through scattering (Warren 1982). The scattering of solar radiation at the snow surface can be divided into 3 different types of processes: single, multiple and

volume scattering. In single scattering, the incoming radiation is reflected directly back to the atmosphere. Multiple scattering refers to the scattering of radiation from one flat particle surface to another and in the end back to the atmosphere (Woodhouse 2006). Volume scattering results from the bulk properties of the snowpack (Shi & Dozier 2000). The amount of these depends on the hardness and roughness of the surface (Warren et al. 1998, Nagler & Rott 2000). The rougher the surface is, the more multiple and volume scattering takes place.

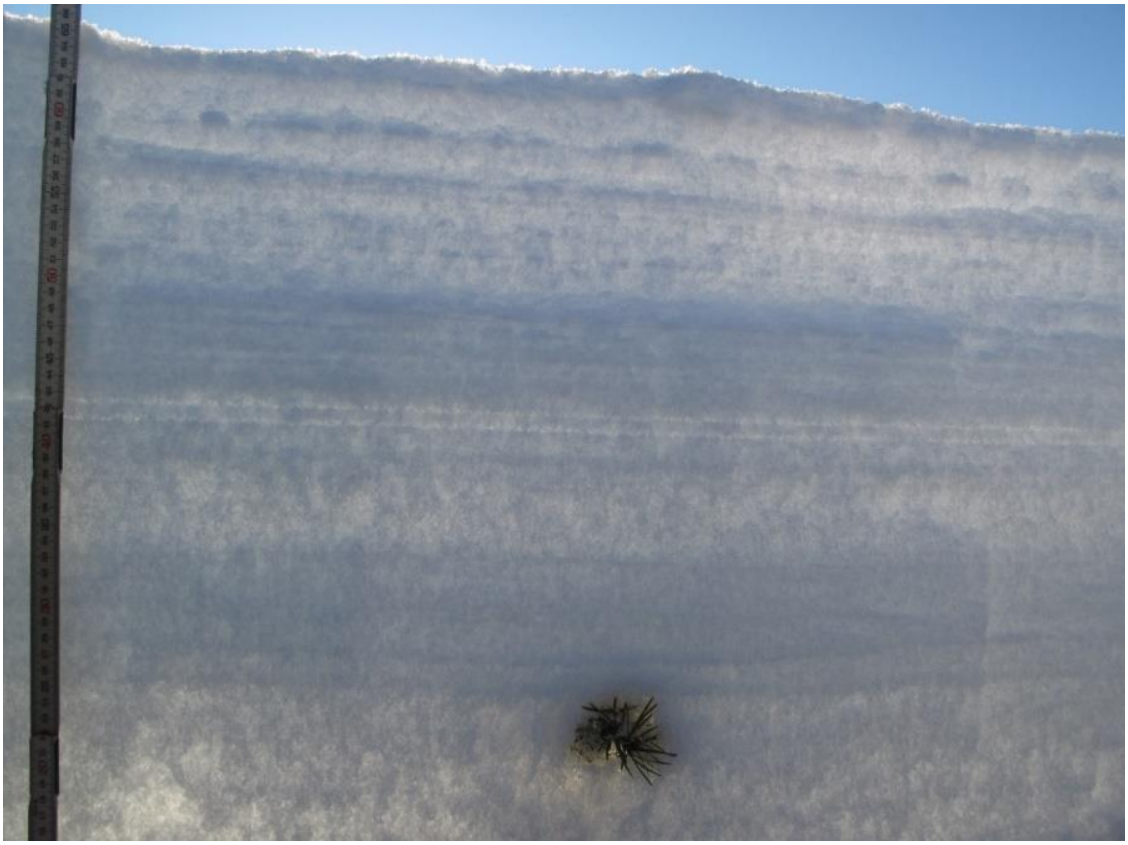

Figure 1 Seasonal snowpack layering at Sodankylä airport 5th April 2013. The photo shows a thin slice of natural seasonal snow (with a small branch of pine (Picea Abies)). The photo was taken by Teemu Hakala, FGI.

In climate studies, the brightness of the earth's surface is typically parameterized by surface albedo. It describes the fraction of the incoming solar radiation that is reflected back to the atmosphere and potentially to the space from the earth's surface. There are different ways to define surface albedo depending on the range of wavelength and the angular distributions included. The albedo used in the study presented in chapter 5.1 is the directional –hemispherical reflectance (so-called black-sky albedo, α_{bsa}) of a given area on the surface describing the incoming solar radiation from one direction, versus the

reflected radiation in all directions, mathematically written as (Schaepman-Strub et al., 2006)

$$\alpha_{bsa}(\theta_s, \emptyset_s) = \int_0^{2\pi} \int_0^{\pi/2} \rho(\theta_s, \emptyset_s; \theta_v, \emptyset_v) \cos(\theta_v) \sin(\theta_v) d\theta_v d\emptyset_v \quad (1)$$

where (θ_s, $\emptyset_s$) are the vertical and horizontal direction of the incoming radiation (a single incident direction),(θ_v, $\emptyset_v$) are the viewing directions of the reflected radiation in the zenithal and azimuthal planes and ρ is the reflectance.

The albedo values of different surfaces vary considerably. Liquid water, such as oceans and lakes have very low albedo values typically around 10 percentage units (Jin et al 2002). Fresh clean snow surface, on the other hand, can have albedo values of up to 90 % (Warren 1982). The albedo of snow depends on the snow surface crystal type, size and distribution on the surface, the scale and directionality of the surface features (surface roughness), impurities, amount of liquid water, Sun and observation angles, and wavelengths in question (Warren 1982, 1984, Warren & Brandt 1998). The most important factor determining the albedo of the snow surface is the grain size (Warren & Wiscombe 1980, Wiscombe & Warren 1980). The albedo values decrease as the grain size increases (Wiscombe & Warren 1980), which explains the darkening of snow surface as the snow ages. There are several methods developed to automatically derive snow crystal size (Ingvander et al. 2012, 2013, Pirazzini et al. 2015). Many of them are based on photogrammetry, where crystal size is derived automatically from crystal images. Also other ways have been developed to describe the effect of snow surface grains on snow optical properties. One of these is specific surface area (SSA), which describes the surface area of the grain per unit mass (Gallet et al. 2009, Gallet et al. 2014).

As the snow starts to melt the grains size and amount of liquid water in the snow increases. This leads to lower values of surface albedo. With the darkening surface the amount of solar energy being absorbed by the snow surface increases, further enhancing the melt and decrease of the albedo. This phenomenon is called the ice-albedo feedback (also known as snow-albedo feedback) (Arrhenius 1896, Budyko 1969, Warren & Wiscombe 1980). The albedo of snow is also affected by surface roughness. So far most of the studies concentrate on large scale roughness, such as sastrugis and smaller scale wind induced formations (Leroux & Fily 1998, Warren et al. 1998, Kuchiki et al. 2011, Zhuravleva & Kokhanovsky 2011). For none-smooth snow surfaces where surface roughness is randomly oriented the albedo is smaller for rougher surfaces due to trapping of radiation in the troughs (Warren 1982). For regular surface features the effect of surface roughness depends on the direction of the Sun relative to the surface features.

Besides the snow geophysical factors, the albedo of snow also depends on the Sun elevation angle, impurities, and cloudiness (Warren 1982, 1984). When clouds are absent, the albedo of a smooth horizontal snow surface increases with decreasing solar elevation. This is due to the likelihood of near horizontal radiation to escape the snow surface instead of being absorbed by the surface. The grain shape becomes more important as the solar elevation decreases, and at low solar elevations the albedo of faceted grains is higher than for other types of grains (Choudhury & Chang, 1981). On cloudy weather, the albedo can be higher than with clear skies due to the multiple scattering of light from the clouds. (Wiscombe & Warren 1980). At the wavelengths where snow exhibits significant absorption, the albedo of a snow surface is higher at lower solar elevations (Wiscombe & Warren 1980, Pirazzini 2004).

The optical properties of seasonal snow depend on several different factors. These include the physical structure of the snow pack, such as crystal size and shape, amount of liquid water and air and the impurities of the snow pack. They contribute to the basis for the surface roughness of the snow, which is discussed in more detail in the following chapter.

3. SURFACE ROUGHNESS OF SEASONAL SNOW

Surface roughness affects the optical properties of seasonal snow. The roughness depends on several different processes and environmental conditions. Some of these are global, (e.g. sun elevation, maritime/continental climate, vegetation zone…) and some are local (e.g. prevailing wind direction and speed, amount and type of precipitation, distance to the canopy...). The dominant factors affecting the surface roughness depend on the scale and environment. At the microscale, the crystal shape and distribution determine the roughness. These depend on the type of crystals that fall on the surface and the metamorphosis of the snow crystals, as described in the previous chapter. In climates where air (surface) temperature stays much colder than the freezing point, the surface features and metamorphosis of snow crystals are mostly affected by reshaping and rearranging of the crystals by aeolian processes. In climates where air temperature rises near or above melting point also sublimation, melting, and refreezing of the snow crystals affect the surface features (Sturm et al. 1995).

At larger scales, the surface features are caused by wind, melting and the topography of the ground. The redistribution of particles by wind modify the crystals and determine the accumulation patterns on the snow surface (Mellor 1965, Jaedicke et al. 2000), such as wind induced ripples and dunes. The macro scale roughness includes also features caused by other factors such as topography, land use and canopy type (Winkler et al. 2005, Deems et al. 2006, Schirmer & Lehning 2011, Eveland et al. 2013, Gruenewald et al. 2013, Scipión et al. 2013, Veitinger et al. 2013). The vicinity of tree trunks affects the surface in a complex way. Forested sites have milder diurnal temperature variation and lower wind speeds than open areas. In open areas wind is often the dominant process affecting the distribution of snow (Lehning et al. 2008) whereas forests tend to attenuate the weather extremes, keeping the air warmer during cold condition and shadowing the surface from direct warming of solar radiation in the spring. This results in slower melting in the spring in forested sites. Trees also affect the distribution of snow. Next to tree trunks under the large branches snowpack is typically shallower. On the other hand, smaller trees with fewer branches can enhance snow accumulation at the root of the tree trunk as the tree trunk acts as a snow fence. At forested sites snow gathers also on the trees. Eventually this snow will fall down to the snow surface causing surface features of different scales. The small particles from vegetation, such as branches and old dried leaves and needles, fall on the snow surface, forming scars and enhancing the melt in the springtime.

Surface roughness and the amount of liquid water are the main parameters affecting the microwave backscatter from wet snow (Williams & Gallagher 1987, Nagler & Rott 2000). The microwave remote sensing data is particularly important in the Polar Regions, where winters do not have enough sunlight and the weather is often cloudy. Also, the bidirectional reflectance distribution function (BRDF) of snow is heavily affected by surface roughness (Warren et al. 1998, Peltoniemi et al. 2010). Therefore, understanding the effect of surface roughness on remote sensing signals on snow-covered surfaces could enhance the quality of both optical and microwave remote sensing based snow and albedo information and enhance the quality of remote sensing based products and climate models.

Seasonal snow surface roughness is a result of several different environmental processes, with different processes being the dominant influence on different scales. The importance of surface roughness on the optical properties of snow surfaces are recognized but the detailed description of the relationship between small scale surface roughness and albedo is still fairly poorly known, with most of the work focusing on the large scale roughness. The understanding of surface roughness would require methods to measure it and large data sets. Examples of these are presented in the following chapters.

3.1. SURFACE ROUGHNESS PARAMETERS

Several different parameters have been developed for describing surface roughness (Church 1988, Manninen 2003, Manes et al. 2008, Fassnacht et al. 2009a, a good overview in Dong et al. 1992, 1993, 1994a, 1994b). The choice of parameters depends on the surface features relevant to the application and the material that is described.

For snow, there are two main fields interested in surface roughness: The studies on the atmosphere-surface interactions describe the surface roughness by using atmospheric roughness length. This is the parameter used in most surface-atmosphere models. It describes the height above the surface at which the mean wind speed reduces to zero when extrapolating the logarithmic wind speed profile down through the surface layer (Manes et al. 2008, Gromke et al. 2011). The roughness of the snow surface affects the wind speed near the surface. This, in turn, affects the exchange of chemicals between the snow and the atmosphere, and the latent and sensible heat flux between these two. The studies on snow surface scattering properties describe the surface by geometric roughness. These include studies on the brightness of the snow surface, scattering modeling of snow, and optical and microwave remote sensing.

The geometrical roughness of snow surfaces is typically described using correlation length and root mean square height variation (σ_h). The values of these parameters depend on the measured scale and the orientation (Manninen et al. 1998). For example, in remote sensing, the surface radiative properties are affected by the roughness from the used wavelength up in fractions of the used scale (Ulaby et al. 1982, Fung 1994, Rees & Arnold

2006). Therefore also the measurements and parameters should describe all the scales that are relevant (Keller et al. 1987, Church 1988, Manninen 1997a, Manninen et al. 1998, Fassnacht & Deems 2006). So far, most of the existing surface roughness studies are made in different scales, directions, and resolutions, which makes it difficult to compare them. Furthermore, most of the existing studies have measured only a single scale, and are thus not fully able to describe the surface. Some multiscale parameters have been developed (Manninen 1997a, 1997b, 2003, Davidson et al. 2000, Löwe et al. 2007, Manes et al. 2008, Fassnacht et al. 2009a), but the directionality has not been taken into account in the parameters as often (Herzfeld 2002, Trujillo et al. 2007).

The parameters used in the papers I-III are based on the root mean square height variation (σ_h), which is a typical descriptor of surface roughness in microwave surface backscattering models (Ulaby et al. 1982, Fung 1994). Since these depend on the measured length (scale), the σ_h is calculated as a function of measured length. The σ_h of a single scale was replaced by the mean σ_h of all the subprofiles of equal length along the whole profile (similarly to the sliding window technique). The σ_h of each profile is calculated using the following equations:

$$\langle \sigma_{h_i} \rangle = \frac{1}{(n-in_0)} \sum_{j=1}^{n-in_0} \sigma_{h_{ij}}, \qquad \mathrm{i} = 1, \dots, n_i \tag{2}$$

where $\sigma_{h_{ij}}$ is the rms height of a subprofile of in_0 points. The size of the smallest subprofile is n_0 and it is enlarged with an increment of *i* so that the size of a subprofile is in_0, where *i* = 1,…,n_i and n_i is the number of different subprofile lengths. The subprofile is moved from the beginning of the whole profile by an increment of *j*. The total number of points in the 1 meter profile is *n*.

According to Keller et al. (1987), for natural surfaces the logarithm of the rms height variation σ_h is linearly dependent on the logarithm of the length *x* for which it is determined, giving:

$$\sigma_h(x) = e^a x^b \tag{3}$$

where *a* and *b* are constant parameters. These parameters will be used in the analysis presented in chapter 3.4.

The parameter values are affected by the inner and outer scale effect. In the inner scale effect, the low number of points in each subprofile or causes statistical uncertainty. In the outer scale effect, the low number of subprofiles has the same effect. The outer scale effect starts to influence the data at subprofile lengths longer than 60% of the maximum length (Manninen et at. 1998). Therefore the analysis in paper II is made using the values for *a* and *b* at 60% of the maximum profile length.

The parameters presented here give means to describe seasonal snow surface roughness in a way that takes into account all measured scales. This is important for scattering modelling, which typically include single input for describing surface roughness when in fact the roughness affects the scattering on many scales.

3.2. METHODS FOR MEASURING SURFACE ROUGHNESS OF SNOW

The studies on snow surface roughness are relatively few. One of the reasons for this is the difficulty of measuring it. Lacroix et al. (2008) have put together an overview of the history of snow surface roughness measurements. Many of these are based on inserting a plate partially into the snow and measuring a profile of the snow surface. These plate-based measurements started in the 1980's by Rott (1984) and Williams et al. (1988). After this, the methods have improved regarding accuracy and resolution (Rees 1998, Rees & Arnold 2006, Löwe et al. 2007, Manes et al. 2008, Elder et al. 2009, Fassnacht et al. 2009a, 2009b, Gromke et al. 2011, paper I). Some of these methods are manual in the sense that the height variation is measured using, for instance, a ruler (Rees 1998) and some incorporate photography (Löwe et al. 2007, Manes et al. 2008, Fassnacht et al. 2009a, paper I). The different methods have been used to measure different types of snow, such as melting snow or freshly fallen snow.

In addition to the plate-based measurements, there are some methods that are based on laser scanning. Most of the methods have measured individual profiles but laser scanning data could be used to cover larger 3-d areas of the surfaces. In addition to improving the accessibility and spatial and statistical coverage, laser scanning gives the potential for studying the directionality of the height variation. It also leaves the surface intact, which gives the possibility to repeat the measurements at the same areas at different times. Then again, this data does not have as high resolution or accuracy as some of the plate methods. More details on laser scanning are given in chapter 4.

In this dissertation, two methods for measuring snow surface roughness are presented. One is based on plate photography, and it is described in detail in the following chapter. It was used in the field in Sodankylä, Finnish Lapland, and the snow profiles were extracted using a fully automatic algorithm developed by Manninen et al. (2012). The results of the

analysis of these profiles are presented in chapter 3.4. The other method is based on mobile laser scanning (MLS), and it is presented in chapter 4.3.

3.3. PLATE PHOTOGRAPHY METHOD

The method used in papers I-III is based on photographing a 1.06 m x 0.4 m wide black board with scales on the sides (Figure 2). The black area in the middle is 1 m x 0.4 m. The scales consist of three rows of black-and-white squares of 1, 5 and 10 mm in size.

While measuring, the plate is carefully inserted into snow so that the top of the plate remains above the snow (Figure 3). The plate is photographed perpendicularly using a Canon PowerShot G10 digital pocket camera. The camera has a 4416 x 3312 pixels and a zoom lens with an optical image stabilizer. One image is enough for retrieving the profile, but to ensure good image quality, three images were taken from each profile. The resolution of the images and the profiles depend on how close to the plate the photograph is taken, but was on average 0.27 mm.

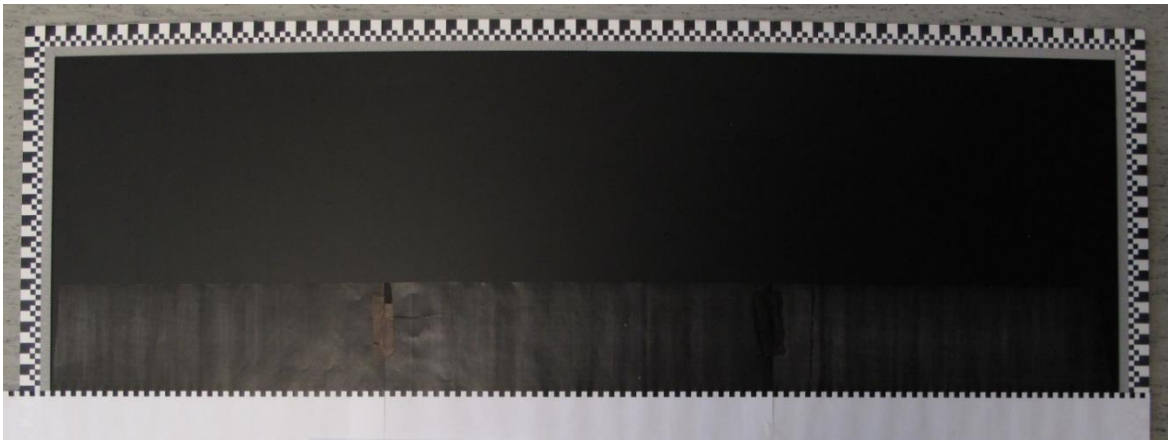

Figure 2 The background used in the plate photography method for measuring snow surface roughness. The calibration of the plate method was made using an artificial tooth rack profile shown in the figure.

The plate and camera are easy to carry during field measurements. Therefore it can be used in a wide area. It can also be taken to the areas surrounded by trees, which can be a limiting factor for the laser scanning based methods, where the tree trunks limit the visibility of the snow surface. The limits to the use of this method come from the resolution of the camera. Also, in some cases, if the snow is loose or has an icy cover, inserting the plate into the snow and holding it in place without disturbing the snow surface profile can be difficult. However, for most cases in the boreal forest zone this is

not the case. Snowfall can also be a problem to the method because falling snowflakes appear as white spots on top of the black plate. These can still be analyzed with little manual assistance, but if the falling flakes appear on top of the snow profile or at the corners of the black area the profile extraction will not be successful.

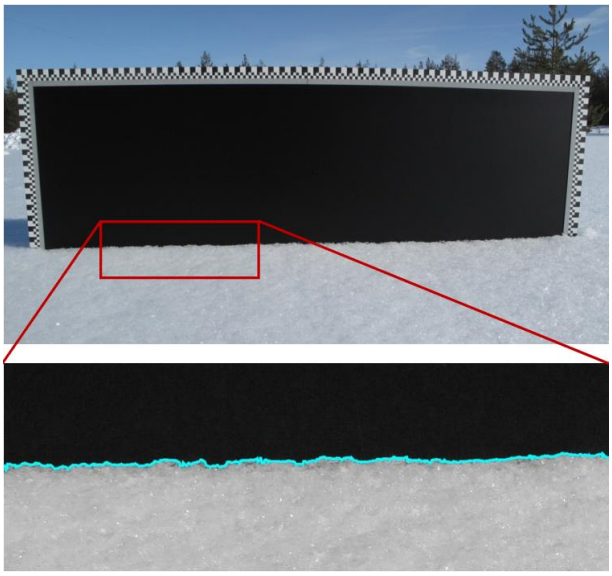

Figure 3 Plate photograph with enlargement of the extracted profile. The profile is from Tähtelä, site index 10, 16th March 2010 with fresh snow.

The vertical accuracy of the coordinates of the profiles was tested by taking a photograph of a straight horizontal paper edge and analyzing it with the method described above. The average absolute deviation of the measured height variation from zero was 0.93 mm with a parabola shape ($y = 0.0000144 \infty^2 - 0.01479x + 2.609$; $R^2 = 0.99$). This is most likely due to the scales of the board being 1 mm above the black background. It may also be due to residual error from the barrel distortion correction. When the coordinates were corrected according to the parabola the absolute deviation of the coordinates from zero was 0.07 mm.

The vertical and horizontal accuracy was studied in more detail by taking photographs of an artificial profile with rack-tooth pattern (Figure 2). The rack-tooth pattern dimensions were 5 mm x 5 mm. The test data consisted of 50 images taken from different angles and distances. From this, a subset of 30 profiles was chosen to represent the realistic measurement settings. The profile was placed on top of the image in different angles for different cases. This dataset was used to construct a residual barrel distortion correction. Based on the rack-tooth –profile analysis the overall horizontal analysis is on average 0.1 mm, with 80% of the cases having an error smaller than ±0.6 mm. The overall vertical accuracy in on average 0.04mm with 80% of errors in a range smaller than ±0.2 mm.

The repeatability of the method was tested by analyzing three different images taken from the same set of the rack-tooth profiles. Twenty-one of the cases had three successful images and were included in the analysis. The profiles were analyzed using root mean square height variation of subprofiles of different length at different parts of the profile (similar to sliding window technique). The mean values of rms height variation for each length of subprofiles were calculated. The subprofiles longer than 60% of the maximum length were obtained from the analysis because the mean value of the longer subprofiles is calculated from only a few individual subprofiles, thus causing statistical uncertainty (Figure 5 in Manninen et al. 1998). The standard deviation of the rms values per measurement is <0.02 mm. The variation of the rms height measurement is typically <1% of the mean value.

The effect of the temperature variation on the dimensions of the scale was estimated to be <0.1 % for a typical measurement temperature range. The detected reasons for the failure of automatic analysis are blurred or out-of-focus images, a very large dark object at the front of the image, snowflakes at the corners of the black area and on scales, and extremely poor contrast of the image intensity.

The plate photography –based method presented here is able to describe the snow surface roughness in scales smaller than 1 m with resolution less than 1 mm. The method is easy to use also in field conditions: it is light to carry, does not require complicated or expensive technical device, and it tolerates moisture and cold weather. Therefore it offers means to gather large data sets on roughness in many different conditions.

3.4. PLATE METHOD RESULTS

The snow surface roughness measurements presented in this dissertation were made as part of the SNORTEX (Snow Reflectance Transition Experiment) campaign (Roujean et al. 2010, Manninen & Roujean 2014). The campaign took place in Sodankylä, Finnish Lapland (67.4°N, 26.6°E) during winters 2008-2010. The base of the campaign during field measurements was in the premises of Finnish Meteorological Institutes Arctic Research Centre (FMI-ARC). The campaign was led by FMI and Météo-France. Also the Finnish Geodetic Institute (FGI, now Finnish Geospatial Research Institute of National Land Survey of Finland), University of Helsinki, University of Eastern Finland, the Laboratoire de Glaciologie et Géophysique de l´Environment, and the Finnish Environment Institute. The campaign aimed at studying the different factors affecting the boreal forest albedo during the melt seasons. It included both airborne and ground-based measurements.

The surface roughness plate measurements made during the SNORTEX-campaign were analyzed using the multiscale parameters developed by Manninen (1997b, 2003, see chapter 3.1). The aim of the study was to gather information on the snow surface roughness of the study area and to investigate the use of the plate-based method and the parameters in question in describing the seasonal snow surface roughness. The

measurements covered different types of natural snow, including fresh, old, wet and dry snow. The measurements cover different types of land use, including forests, open bogs and lake ice (Figure 4). The plate profiles were analyzed using the parameters *a* and *b* (Eq. 3)

The parameter *a* and *b* (Eq. 3) react differently to the features along the profile they describe. Parameter *a* reacts to the height variation of the shorter wavelengths. Therefore fresh fluffy snow gets high values of *a*, and aged snow gets lower values correspondingly. The parameter *b* reacts to the longer wavelength characteristics and irregularity of the occurrence of height variations. The surface features of older snow have less variation in the crystal level, but larger variation in the longer wavelengths. This variation is caused by melting, impurities, and scars made by animals on top of the snow. These are more irregular in nature than the wind induced ripples or crystal level features and therefore old melting snow gets high values of *b.*

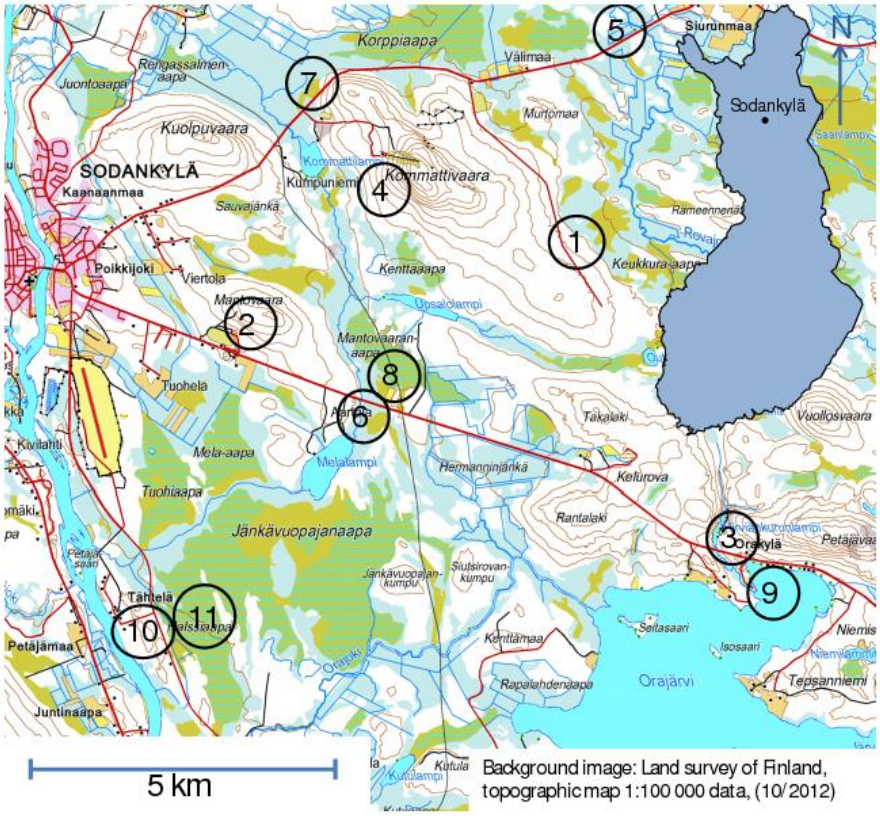

Figure 4 *The measurement sites for plate photography measurements during SNORTEX campaign.*

The different character and sensitivity of the parameters can be seen in Figure 5. The figure presents the values for *a* and *b* for all measured profiles. The parameters from the

March 2009, February 2010 and March 2010 profiles show similar combinations for the values for the two parameters but the profiles measured in April 2009 form a separate group of values. This is because April 2009 was melt season whereas the other months did not yet experience as much melting. For April 2009 the values for *b* are generally higher for the corresponding values for *a* than for the other months. This is because in the melt season the new fresh snow is not able to level out the irregular pits and peaks of the already melting snow surface.

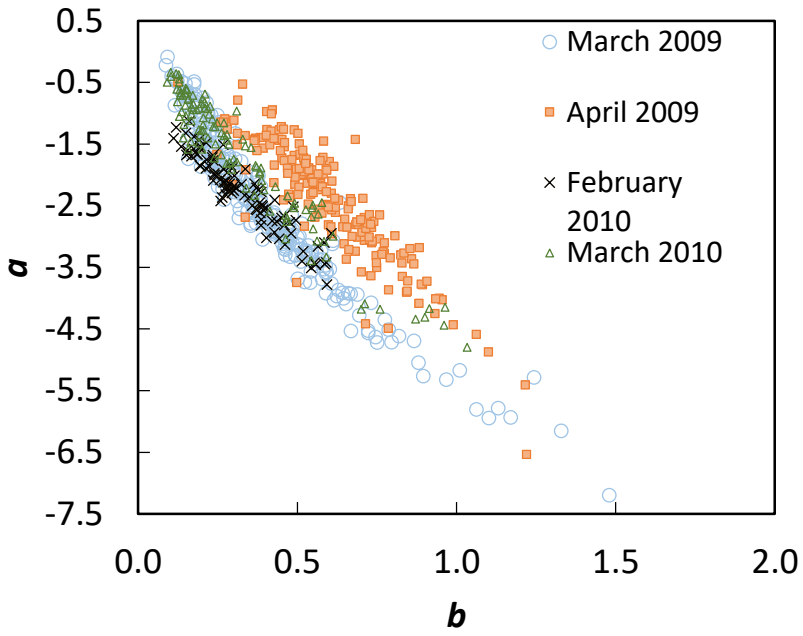

Figure 5 The parameters a and b of Eq. 3 for 60% of the maximum length for all plate profiles from 2009 and 2010.

The effect of a single snowfall event on the values for parameter *a* can be seen in Figure 6, which shows the values for the two parameters for Tähtelä (site 10 in Figure 4) for March and April 2009. At the beginning of the field campaign in March 2009 the snow surface was aging. At the evening of 15th March, it began to snow, continuing in short periods until the morning of 18th March. This can be seen in the values for parameter *a*, which gets relatively low values at the beginning of March 2009. Then, as the snowfall starts, the values increase, and after the snowfall they gradually decrease. The values for *a* are in the range of -4 to -0.5. This is also the range of values for *a* in all the measurement sites in March 2009. This shows that the weather conditions can largely explain the distribution of *a*. In April 2009 there was no snowfall during the measurement period.

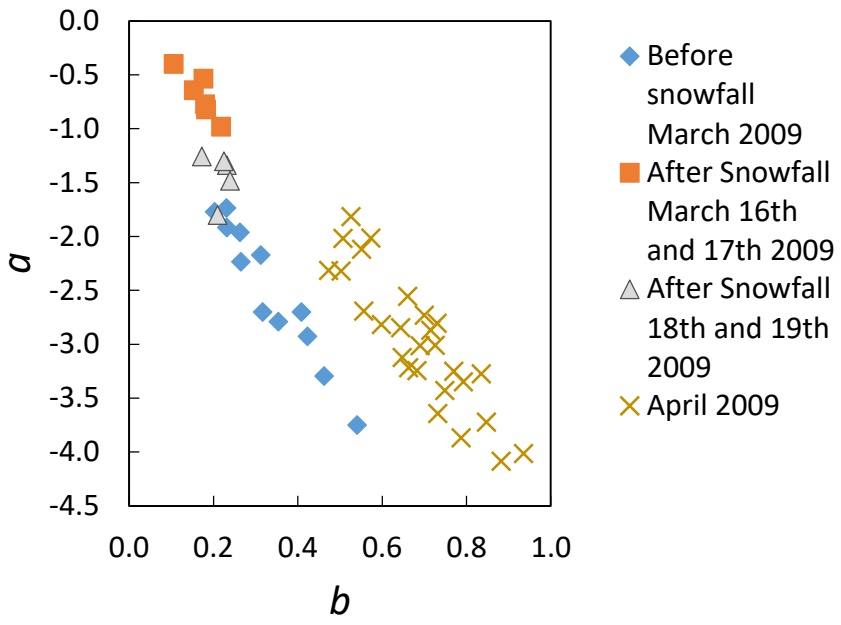

Figure 6 The temporal variation of parameters a and b of Eq. 3 in Tähtelä from 11th March 2009 to 28th April 2009.

The results here present a large data set of small scale surface roughness measurements. The measurements cover many different types of environments and thus snow types of the Boreal Forest. The parameters used here were able to distinguish between old and fresh snow surfaces, as well as the difference between mid-winter and melt season snow. Previous studies have shown that the albedo of snow decreases as the snow gets older. The study presented here shows that the small scale surface roughness changes as the snow gets older. This suggests that the small scale surface roughness has an effect on surface albedo.

4. LASER SCANNING OF SNOW COVERED SURFACES

Laser scanning is a technique ideal to use in 3D mapping of different targets, such as topography, forest, vegetation, buildings and indoors areas. It has proven to be particularly good at measuring inaccessible and dangerous environments. It also leaves the measured surface intact, which means it can also be used for change detection.

The applications for laser scanning are rapidly increasing as the scanning systems are becoming cheaper and easier to use. The laser scanning methods can be divided into airborne and terrestrial methods. In airborne laser scanning (ALS) the scanning system is installed onboard an aircraft. These systems can cover large areas, but the resolution and accuracy of the data is not as good as with terrestrial laser scanning (TLS), where the scanner is on ground, typically mounted on a tripod (Rees & Arnold 2006, Van Der Veen et al. 2009, Hollaus et al. 2011). The measurements presented here are made using TLS.

In the recent years, several different methods have been developed, where the scanning system is mounted on a moving vehicle. These mobile laser scanning systems (MLS) cover larger areas than stationary laser scanning and the data has higher resolution and accuracy than the airborne data. The MLS systems typically have a 2-d profiling laser scanner mounted on a moving vehicle, where the movement of the vehicle provides the third dimension for the point cloud. The systems consist of a scanner, a moving vehicle, a GPS-device and an inertial measurement unit (IMU). The MLS system used in the study presented in chapter 4.3 is the FGI ROAMER (Kukko et al. 2007).

Laser scanning is based on the scanner sending a laser beam towards an object or area and then measuring the backscatter of the beam. The direction to which the beam was sent, and the time it took until the photodiode of the scanner detected the backscattered beam gives the location of the reflecting surface. The range measurement can be based either on the time-of-flight or on the phase-based measurement principle. Changing the direction of the outgoing beam the observations can be combined into a 3D point cloud, where the data of each measured point contains x, y and z coordinates and the intensity of the backscattered beam. The 3D point cloud can then be analyzed using either photogrammetric methods to extract different objects or by modeling the surfaces.

The intensity data of a point cloud tells the relative intensity of the backscatter of the laser beam for each measured point within the scan. The data has not yet been used for many applications, but the methods utilizing also this information are increasing. Since the intensity data is gathered automatically while scanning, making it usable for data analysis would bring added value to the work and create new possibilities for applications. For

snow surfaces, this could mean for example automatic classification of snow surface types.

The intensity value of a laser point is affected by the backscattering properties of the reflecting object. With snow, this means the grain size and shape (Kaasalainen et al. 2006) and the surface structure (Zhuravleva & Kokhanovsky 2011). The backscattering properties of the target then affect the angular dependency of the intensity, that is, the incidence angle effect (Kaasalainen et al. 2011, Krooks et al. 2013). The effect of measurement geometry and its correction has been studied by Sicart et al. (2001) and Weiser et al. (2015). Knowing the effect of incidence angle is particularly important for MLS data which typically covers a larger area and thus wider range of incidence angles.

In order to be able to use the intensity value, it needs to be calibrated since the absolute intensity value changes between different datasets. This is typically done using objects whose reflectance is pre-known (Kaasalainen et al. 2009). In field conditions, these can be placed in the view of the scanner and later extracted from the data and used as reference values to calibrate the data. This also enables the comparison of different datasets. Different radiometric calibrating systems have been developed by, for instance, Ahokas et al. (2006), Coren & Sterzai (2006), Höfle et al. (2007), Kaasalainen et al. (2009) and Wagner et al. (2006). Calibrated intensity data has previously been used for range data segmentation and classification (Höfle et al. 2007, Yan et al. 2012).

Using laser scanning on snow surfaces requires knowledge on the behavior of laser beam on the snow surface. The usability of MLS in snow applications was studied by Kaasalainen et al. (2010). Since some types of the snow surface crystals are transparent in the direction of the optical axes of the crystal, and the surface may contain liquid water, there is a chance that the laser beam backscatter does not come from the surface, but from lower levels of the snowpack. Prokop (2008) has studied the depth the backscattering represents by placing reflective foils and blankets on the snow and comparing the range data from the blanket and the snow. According to his study, there was less than 1 cm difference in the surface height of the different surfaces. Here the depth from which the backscattering takes place is studied by placing black metal plates horizontally into the snowpack and observing the effect they have on the intensity value of the backscatter (chapter 4.1).

To be able to use the laser scanning intensity data for snow surfaces several factors need to be taken into account. First, the snow BRDF is highly varying. In stationary terrestrial laser scanning data, the direction of the laser beam changes as the scanner rotates. This means that each laser point observation represents the backscattering for a different angular composition of the BRDF. The incidence angle between the scanner and snow surface changes also along the scan line. The effect of these need to be taken into account while using the intensity data. This dissertation presents a study on the incidence angle dependence of the intensity data from different snow types (chapter 4.2).

In glaciology laser scanning has mostly been used for snow depth measurements and the applications have focused on using the range data (Arnold et al. 2006, Várnai & Cahalan

2007, Kaasalainen et al. 2008, Prokop 2008, Prokop et al. 2008, Hood & Hayashi 2010, Helfricht et al. 2014, Picard et al. 2016). Some first attempts have been made to use airborne laser scanning data for glacier surfaces (Lutz et al. 2003, Höfle et al. 2007). The surface roughness studies using laser scanning have focused on different snow-free surfaces (Lacroix et al. 2008, Eitel et al. 2011). ALS has been used to study the roughness of larger areas, such as ice sheets (Van Der Veen et al. 2009) and forest canopy (Weligepolage et al. 2012). This dissertation presents a study on the feasibility of MLS data on snow surface roughness mapping (chapter 4.3).

4.1. DEPTH OF BACKSCATTER

The depth from which the backscattering takes place was studied by placing black metal plates horizontally into the snowpack and observing the effect they have on the intensity value of the backscatter. As soon as the intensity value starts to change the laser beam has reflected from the depth of the plate. The measurements were made using Leica HDS6100 scanner. It measures at 650-690 nm wavelength. The beam diameter at exit was 3 mm, having a beam divergence of 0.22mrad. The range measurements were based on phase detection. Additional measurements were made with a Sick LMS151 laser scanner to compare the results of the phase-based scanner with the pulse-based one. The Sick scanner measures at 905 nm wavelength and has an 8 mm beam exit with15 mrad beam divergence.

The intensity detector of the Leica scanner is linear and follows the R_l^2 dependence (R_l being the range) of the radar equation (Wagner et al. 2006) at distances greater than 10 m (Kaasalainen et al. 2011):

$$P_r = \frac{P_t D_r^2}{4\pi {R_l}^4 \beta_t^2} \sigma_b \quad (4)$$

where P_r is the received power, P_t is the transmitted power, D_r is the receiver aperture, R_l is the range, and β_t is the transmitter beam width. σ_b is the backscatter cross section, which is related to target reflectivity and the measurement geometry. In this study, all parameters, including the range R_l, remained constant, except for σ_b, which depends on the incidence angle (cf. Shaker et al. 2011, Kaasalainen et al. 2011).

According to Höfle & Pfeifer (2007), the σ_b depends on the incidence angle as follows:

$$\sigma_b = \pi \rho R^2 \beta_t^2 cos\alpha_{ia} \quad (5)$$

where ρ is the target reflectance, R_l is the range, β_t is the laser beam width and α_{ia} is the incidence angle. With plates in the snowpack closer than where the backscattering would take place, it would affect the surface reflectivity, which is also contained in the cross-section parameter σ_b (Wagner et al. 2006).

The measurements were made at the premises of FGI in Kirkkonummi (60.1°N, 24.5°E), Finland. The snow cover in this region is typical taiga snow with ice lenses and several layers with different density and crystal shape (Sturm et al. 1995). The relevant geophysical properties of the snow were documented and the overall weather conditions, such as air temperature, were monitored during the measurements.

The snow cover was studied using standard snow pit measurements. After this, a clear cut in the snowpack was made, and black aluminum plates were inserted into the snow at different depths in a horizontal position similar to the snow surface (Figure 7). The plates were 50 cm x 25 cm and 15 cm x 10 cm in size. The bigger plates were used deeper in the snowpack to ensure that they cover the sample area. The smaller plates were used near the surface where the snow was less packed and therefore inserting the plates into the snow without destroying the surface was more difficult. They were also easier to place at an exact depth.

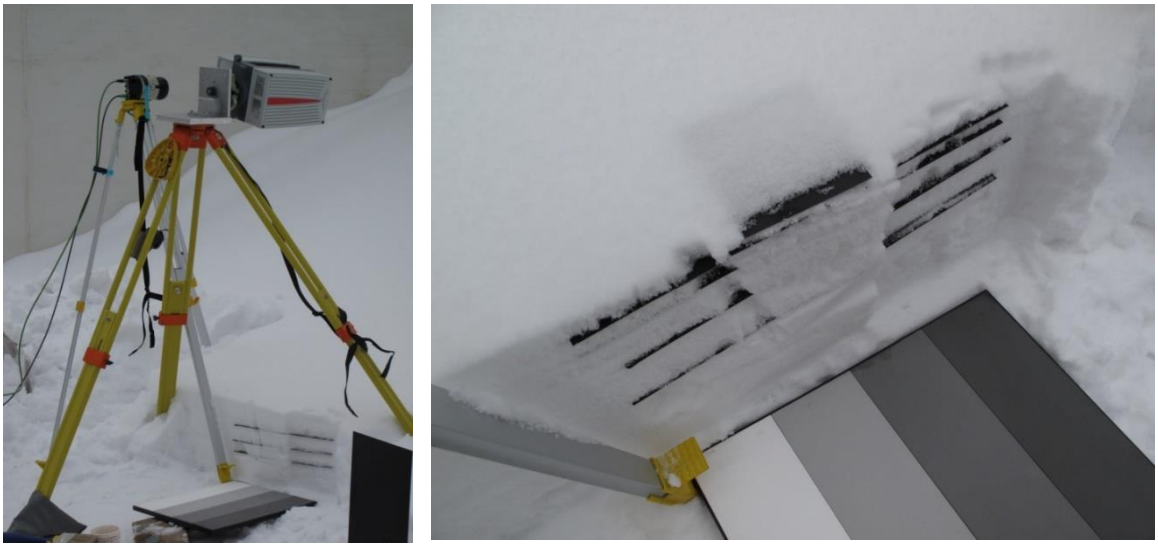

Figure 7 The set up for measuring the depth of backscatter. Left: The scanners were placed above the snow surface (here both Leica on the right and Sick on the left). Right: The Spectralon® reflectance panel was placed in the view of the scanner and black metal plates were inserted into the snow.

The scanner was placed so that the incidence angle was as close to perpendicular to the surface as possible. A Spectralon® reflectance panel was placed in the view of the scanner next to the snowpack (Figure 7). The first scanning was done without plates, followed by the case where the plate was at the deepest (typically 20 cm depth). In order to not break the snowpack, the plate was left in the snow and a new plate was placed above it. The closer to the surface the plates were, the less difference there was between the depths of different plates. Near the surface, the scanning was made at 0.5 cm depth interval. After collecting the data, a sample of the laser scanning data from the snow surface above the plates was extracted from the point cloud and the differences in the intensity values from samples of different plate depths were compared. The typical sample size was 10 x 10 cm.

The measurements were repeated on different days with different types of snow. The snow types covered fresh fluffy dendritic snow to old wet slushy snow. Images of the different snow surface crystals together with the weather data are seen in Table 1. If the snow was scanned from a too short distance there would be a risk of oversaturating the intensity values. Therefore the scanning was carried out from different locations as straight above the snow sample as possible but still far enough.

The mean normalized intensity values for measurements of different snow types with plates at different depths are shown in Figure 8. The values are normalized using the mean intensity value of the 99 % backscattering plate of Spectralon® reflectance panel. According to the measurements for dry snow, the backscattering takes place from the very surface of the snow. The results were similar to the results obtained by the Sick scanner. For wet snow, the black plate starts to affect the intensity values already at 0.5 to 1 cm depth. This indicates that the majority of the backscatter comes from this depth. Since natural snow is not a featureless plane the depths of the black plates should be considered as approximate.

The use of laser scanning on describing snow surface feature requires the understanding the behavior of laser beam on snow surfaces. The work presented above shows that the backscattering of the laser beam takes place at the very surface of the snow.

Table 1 Weather and snow conditions of each day of the backscatter depth measurements: The scales in the crystal images are in cm.

26th January 2012 **Scanner position:** next to the snow, see Figure 3 **Snow depth (cm):** 34 **Air temperature:** -5°C **Surface crystals:** DFbk/PPsd, dendrites, and broken dendrites	
16th February 2012 **Scanner position:** from a window on a higher floor **Snow depth (cm):** 32 **Air temperature:** -2.5°C **Surface crystals**: DFbk, dendrites and broken dendrites	
13th March 2012 **Scanner position:** from a roof **Snow depth (cm):** 30 **Air temperature:** +5°C, half cloudy **Surface crystals:** RGlr, MFcl, large rounded clustered crystals, very wet	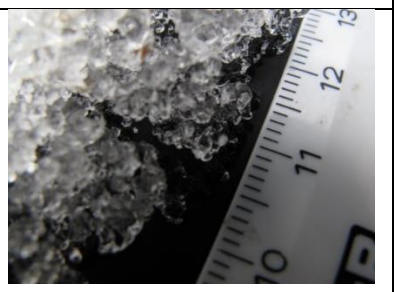
7th February 2013 **Scanner position:** from a roof **Snow depth (cm):** 25 **Air temperature:** 0°C **Surface crystals:** DFbk, wet but fresh, sticky dendrites and broken dendrites	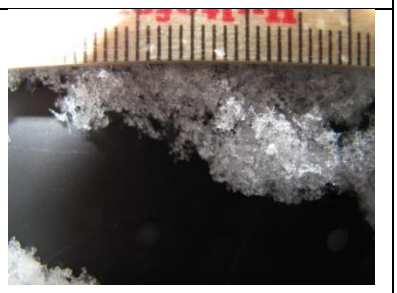
14th February 2013 **Scanner position:** from a window on a higher floor **Snow depth (cm):** 75 **Air temperature:** 0°C, cloudy **Surface crystals:** MFcl, wet rounded clusters, some evidence of earlier freezing with sharp edges	

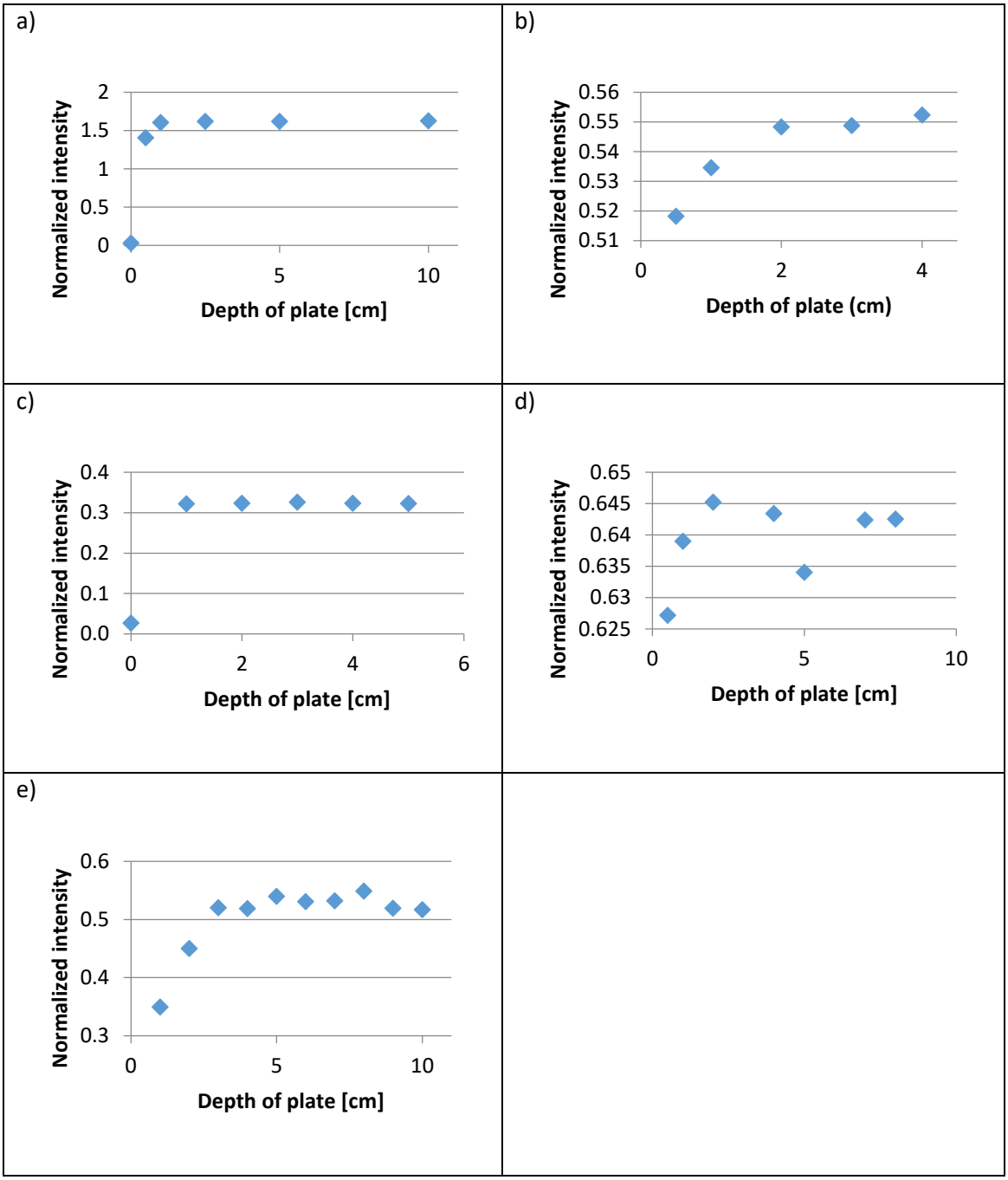

Figure 8 The normalized intensities of the snow surfaces for the different measurements. The measurements were made a) 26th January 2012: dry dendrites b) 16th February 2012: dry dendrites c) 13th March 2012: wet rounded and clustered d) 7th February 2013: wet fresh dendrites e) 14th February 2013: wet rounded clusters. The horizontal axes shows the depths of the plates.

4.2. *THE INCIDENCE ANGLE DEPENDENCY OF THE INTENSITY OF LASER BACKSCATTER FROM DIFFERENT SNOW SURFACES*

The dependence of the incidence angle effect on snow type was measured using the Leica HDS6100 scanner presented in the previous chapter. The wavelength dependency of the incidence angle effect was studied using Hyperspectral Lidar (HSL) developed at FGI (Hakala et al. 2012). During measurements, the scanners were placed indoors in a laboratory and the snow samples were kept outdoors (Figure 9).

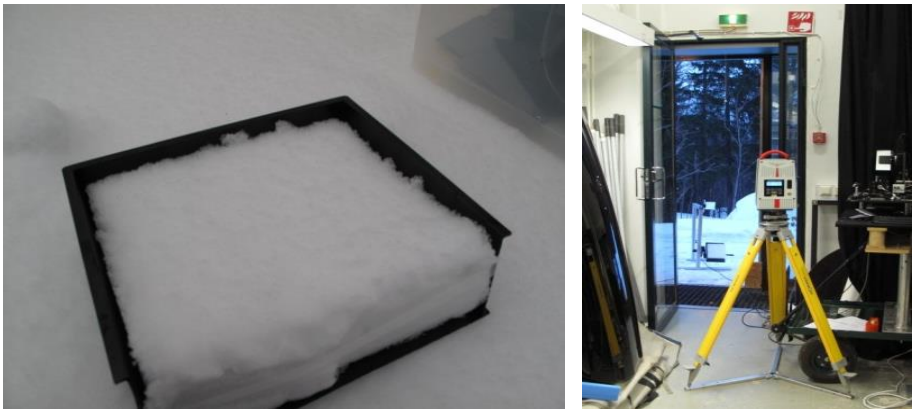

Figure 9 Left: The snow sample of natural snow in a plastic container. Right: The setup for the scanning. The scanner is at the front of the image and the snow sample with the rotator is on the back.

The different snow surfaces were studied by cutting 20 cm x 20 cm samples of different snow surface using a thin plastic box with one side wall open (Figure 9). The samples were 6-8 cm thick. The sample was kept in the same box during the measurements. The box was installed on a URB100CC rotation stage (Newport, Irvine, CA). The rotation device was mounted on an aluminum frame along with a mirror. The snow sample was then scanned several times, each having the sample in a different angle. The distance between the snow sample and the scanner (via mirror) was about 5 m. The mirror was used to enable measurements of greater angles without destroying the snow sample.

The data were analyzed by fitting a plane to the point cloud from the snow sample to measure the incidence angle more precisely. The analysis is based on the mean and median values of the intensity values for the snow sample. A similar set of measurements were made during several days having different snow surface. Snow crystal images together with weather information for the different measurements can be seen in Table 2. The crystals have been classified according to Fierz et al. (2009). Additional

measurements with different wavelengths were made using HSL (Hakala et al. 2012) 21th February 2012. The backscatter was measured at 8 wavelengths (554.8 nm, 623.5 nm, 691.1 nm, 725.5 nm, 760.3 nm, 795.0 nm, 899.0 nm, 1000.4 nm).

Table 2 The weather and snow conditions of the measurements of the incidence angle effect. The number of the scale in the images of the snow surface crystals is in centimeters.

4th February 2013 **Snow depth (cm):** 18 **Air temperature:** 0°C **Surface crystals:** DFdc, broken dendrites and needles, fresh fallen snow	
14th February 2013 **Snow depth (cm):** 41 **Air temperature:** 0°C **Surface crystals:** DFdc, needles and decomposed dendrites, that have partially melted and then refrozen	
21st February 2013 **Snow depth (cm):** 37 **Air temperature:** 0°C **Surface crystals:** DFdc, old broken crystals that have been clustered but are not yet very rounded	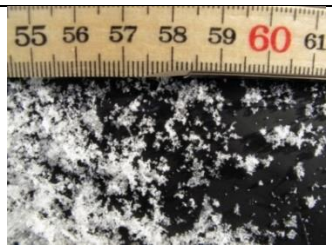
4th March 2013 **Snow depth (cm):** 30.5 **Air temperature:** -5.5°C **Surface crystals:** DFdc, needles and broken dendrites	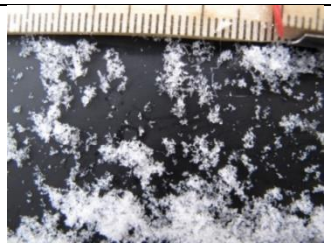
19th March 2013 **Snow depth (cm):** 33.5 **Air temperature:** -6°C **Surface crystals:** DFbk/PPsd, a fresh fluffy layer of dendrites	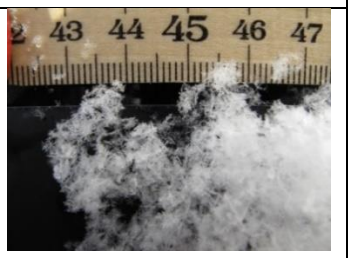

To ensure the stability of the setting during the different scans, a four-step Spectralon® (Labsphere Inc.) reflectance target with 12 %, 25 %, 50 % and 99 % reflectance panels was placed near the snow sample in the view of the scanner. During the data analysis, the 99 % panel was used to monitor the comparability of the different scans. The stability of the measurements was monitored also by measuring air temperature next to the snow sample during measurements, visually monitoring the snow sample between the scans and during the rotation, and sampling the snow point cloud both through the mirror and directly.

The mean intensities for different snow types as a function of incidence angle are shown in Figure 10. The incidence angle dependency seems to be similar to all measured snow types. The differences between the measurements are smaller than the standard deviations of intensity values of the samples. The intensity values where typically normally distributed. Therefore the mean value represents the sample well. The similar dependency of the intensity of the different snow types on the incidence angle gives the possibility to use similar correction function for the intensity values for all snow types. A first-order cosine function for the incidence angle was fitted to the intensity data. Due to the measurement setting the other variables are static. The fitting of the first-order cosine function gives an empirical correction:

$$0.1009 + 0.8812(\cos\alpha_{ia}) \quad (6)$$

The R^2 for the fitting was 0.9884. A more precise fitting needs to be done when a larger data set including wet snow is available. The intensity values for different wavelengths seem to have a similar dependency on incidence angle.

The incidence angle measurements originally included a sample set of wet snow, but the data turned out to be corrupted. Therefore it was excluded from the analysis. It is noteworthy though that the excluded data followed the same pattern as the other snow types. This is in line with the previous experiments including also different incidence angles from wet snow (Anttila et al. 2011).

The results presented above show that the incidence angle dependency of the laser scanning intensity value is similar to all snow types. More similar measurements need to be made in the future to form a more precise correction function for the incidence angle effect. These results will enhance the usability of the intensity data in laser scanning based methods for snow cover mapping.

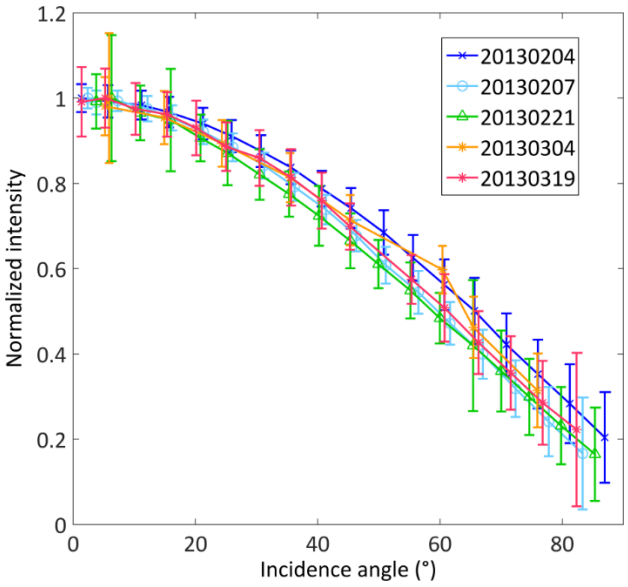

Figure 10 The mean backscattering intensity of the snow samples. The intensity values have been normalized using the maximum values of each measurement set. The error bars show the standard deviation of the snow samples.

4.3. MOBILE LASER SCANNING MEASUREMENTS OF SNOW SURFACE ROUGHNESS

The MLS and validation measurements of seasonal snow surface roughness were made during the SNORTEX campaign 18th March 2010. The scanning was made using the FGI ROAMER system, which includes a FARO Photon 120 laser scanner and a NovAtel SPAN GPS-IMU system, together with data synchronizing and recording devices. A summary of the equipment can be seen in Table 3. FGI Roamer was mounted on a sleigh and driven by snowmobile along a 2.5 km long track (Figure 11 and Figure 12). The track followed a marked snowmobile track and covered sparse pine forest and open bogs. The GPS-IMU system measures the platform movements and observes the GPS satellites to reproduce the system trajectory for the scanner data. The data is recorded as a function of time at 100 Hz data rate. At post-processing, the scanner point data is time synchronized with the trajectory data from the GPS-IMU, producing a 3D point cloud.

The data from 18th March 2010 was surveyed using 49 Hz scanning frequency and point measurement rate of 244 000 pts/s. The scanner head was mounted upwards on the sleigh for vertical profiling to produce across-track swaths. The point density of the data in hand varies between 100 pts/m^2 and 3000 pts/m^2. The spacing between the scan

swaths in the data was approximately 2-6 cm depending on the speed of the vehicle. A sample of the gathered laser data can be seen in Figure 13.

Table 3 Technical details for FGI ROAMER.

Scanner	FARO Photon 120
	120-976 000 pts/s, user selectable
The maximum field of view	320°
Scan frequency	3-61 Hz, user selectable
Wavelength	785 mm
	Phase shift ranging
Spot size	3.3 mm + 0.16 mrad divergence
Georeferencing system	NovAtel SPAN GPS-IMU
	NovAtel DL-4plus receiver and GPS-702 antenna
	L1 and L2 frequencies
	Honeywell HG1700 AG11 tactical-grade RLG IMU
	Gyro bias 1.0 deg/h
	Random walk 0.125 deg/rt-h
	Data rate 100 Hz
Bi-trigger synchronization	
	Delivers scanner triggers to receiver log
	Camera triggering × 4
Rugged laptops for data recording	

Figure 11 The FGI ROAMER mounted on a sleigh, moved by snowmobile.

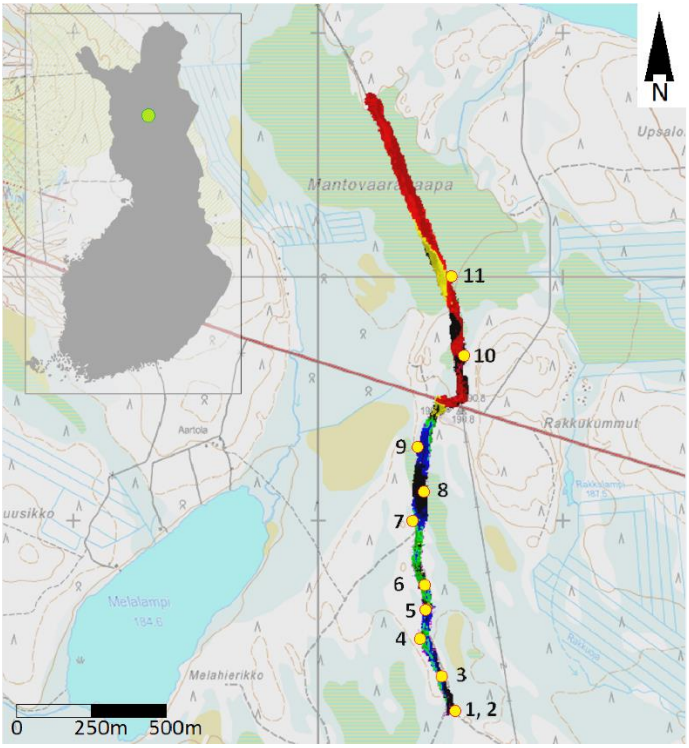

Figure 12 The MLS data coverage for 18th March and plate profile validation sites (yellow dots). Map data courtesy: NLS of Finland.

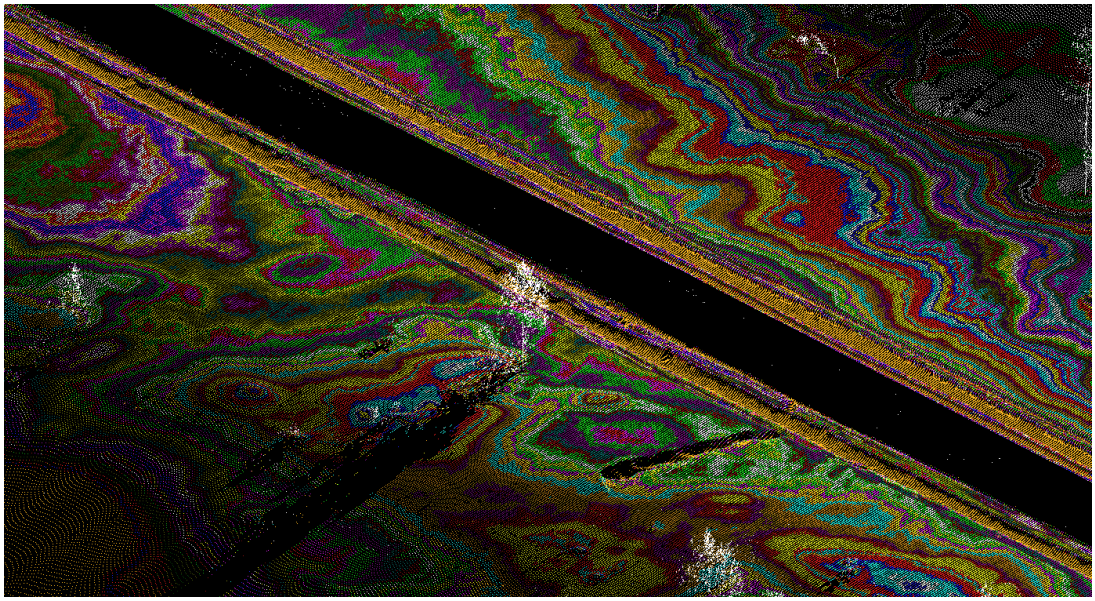

Figure 13 A sample of MLS data from 18th March 2010. The colors come from surface elevation variation. The white objects are trees and the 2.5 m wide black area is the area near the scanner for which data could not be collected due to shadowing of the scanner.

According to the scanner manufacturer, the point measurement accuracy of the scanner is 2 mm with 1 mm repeatability for 90 % reflective target. In practice, however, the accuracy depends on the object surface type, reflectivity and object angle relative to the scanning beam. The relative point accuracy of this system is estimated to be a few millimeters. The absolute positioning accuracy is at centimeter level. The largest source of error in the data is the direct georeferencing of the mapping sensor data with global satellite navigation and inertial positioning.

To study the usability of this data for snow surface roughness mapping, plate measurements of snow surface roughness similar to the ones presented in chapters 3.3 and 3.4 were made along the track. The plate profiles were measured in the same direction as the swath (perpendicular to the scan lines) at 11 locations (shown in Figure 12) shortly after the scanning. Corresponding surface profiles were extracted from the laser scanning data. The profiles were cut using 3 cm and 5 cm wide boxes. The profiles were cut both along the scan swath and perpendicular to it (similar to the plate profile). At some locations, an additional set of profiles were cut from the scanning data closer to the scanner in order to get better resolution for the laser scanning profile. This was done only if the original plate measurement was far from the trajectory and the snow surface between the plate profile and the scanner was intact.

The corresponding plate and laser scanning profiles were compared using rms height variation calculated as a function of measured length (Eq. 2). The linearly rectified profiles can be seen in Figure 14. The profiles can be divided into two groups according to the comparison results: The profiles that match rather well considering the shape and magnitude, and the profiles that do not match quite as well.

The plate profile locations were located from the laser data using distinct visible objects such as placing of tree trunks relative to the profile. In some cases, the laser data turned out to be too sparse for meaningful profile extractions, and the profiles were cut purposely from a different location. This mismatch of locations is also causing some differences in the comparison between the plate and the laser scanning profiles. Some differences are expected to be caused by the fact that the laser scanning profiles show centimeter level roughness, whereas the plates measure roughness with sub-millimeter resolution. At validation site 9 the surface shows a slight bump while at validation sites 3 and 6 there is some wind induced ripples, and the profiles from different sources seem to have been taken at a different phase of the ripple formation. However, for relatively flat and smooth snow surface, such as the one measured here, the variation in scales larger than millimeters is so little, that the miss-locations may not have as large effect on the rms height variation as it could have at different surfaces. This is also demonstrated by the fact that in some cases the laser scanning profiles measured parallel to the plate profiles match the plate profiles even better than the laser profiles measured in the same direction as the plate profile. The surface height variation along the profiles is typically in centimeter scale, as can be seen in the plots in Figure 15, and the scale of variation is the same for both the methods.

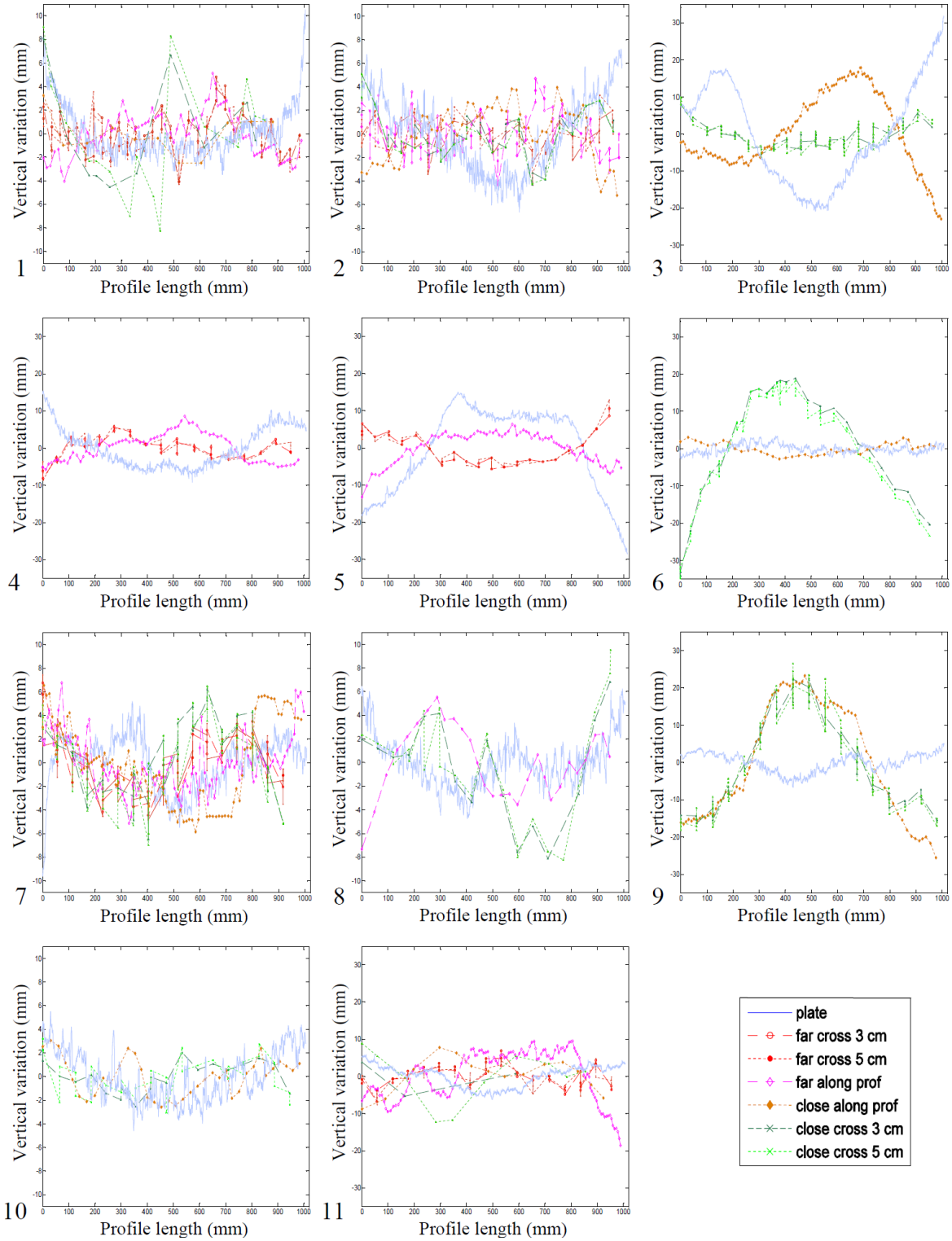

Figure 14 Snow surface profiles derived by using plate photography and MLS. The profiles taken at the same location as the plate profile are indicated as "close" and the profiles extracted further away from the plate profile are indicated as "far".

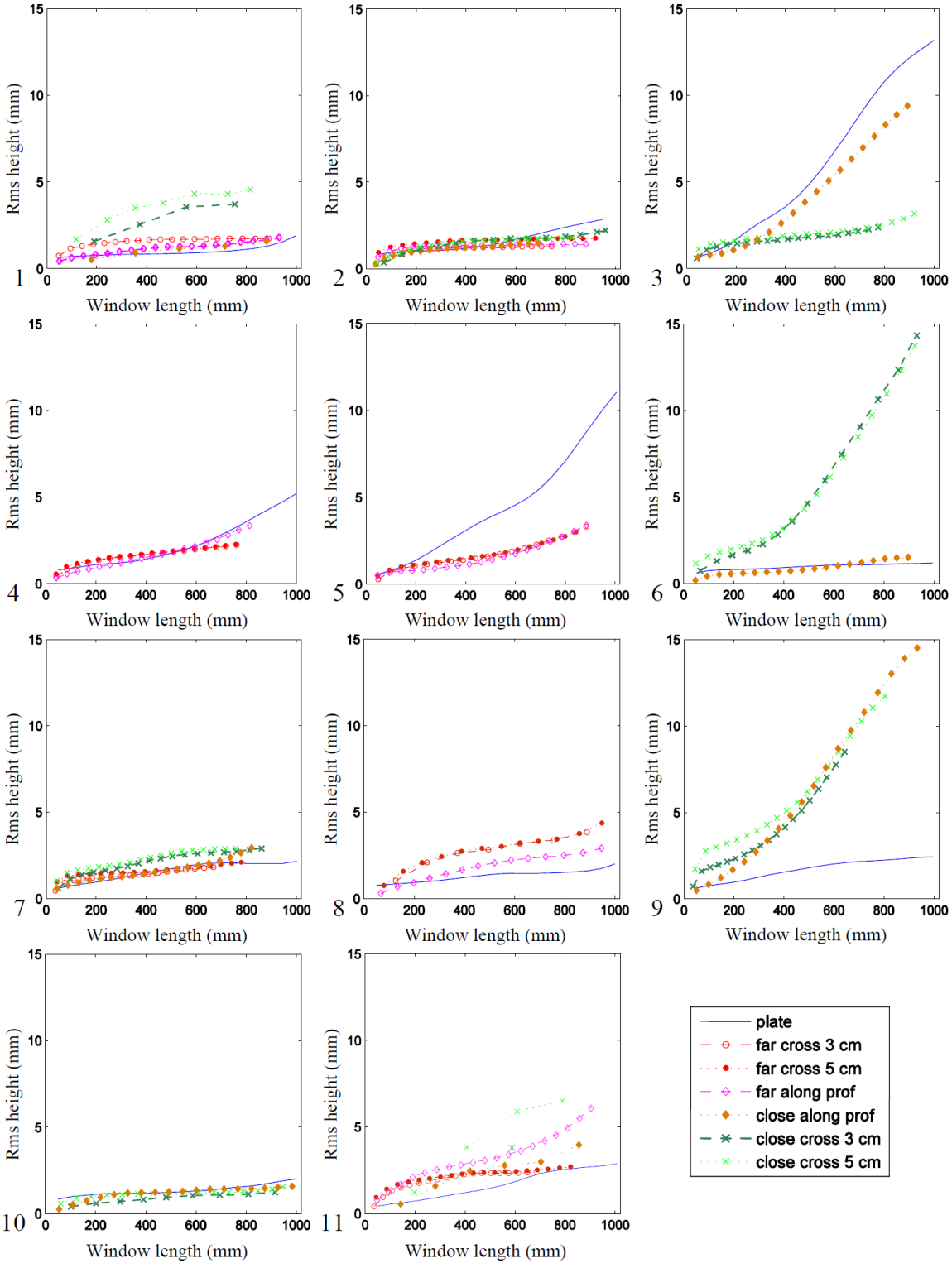

Figure 15 The rms height variation of the MLS and plate profiles.

The resolution of the laser profiles parallel to the laser swath (along scanline) is typically much higher than the profiles that were cut across the swath. The role of resolution, uneven point density, laser spot size, wavelength and function of range and incidence angle on the surface roughness parameters should be studied in more detail. In this study

the laser spot size at the far edge of the snow surface data is about 30 mm, taking into account also the effect of incidence angle. The used wavelength, 785 mm, is so close to optical wavelengths, that the penetration and absorption to the surface are expected to have little effect (Warren et al. 2006). The depth from which the backscattering takes place on snow surfaces is studied in more detail in paper IV. The differences between the rms functions from the two methods are within 2 mm, especially for scales 50-60 cm. In the cases where the differences are larger, they are still on the scale of 10 mm.

After the MLS data was shown to be potential for snow surface, a method to obtain snow surface roughness (MLS grid) by using surface classification and 3D samples was developed. The method starts with cleaning the data from noise points and separating the snow surface from observations of other targets. Points with less than five points within the radius of 20 cm from the point in question were removed. This step caused the removal of some points from snow cover at far distances (greater than 25 m). Therefore, the stray points were not removed directly but classified as “sky points”, giving the possibility to restore them in case they are needed at later application.

After filtering the noise points from the data, the snow surface was extracted from the point cloud. The snow surface classification followed the method introduced by Axelsson (1999). The method starts by building a surface model from points given by the user, in this case, the points still left in the point cloud after cleaning. The model consists of triangles and it is then gradually extended by iteratively adding points to the point cloud. A set of parameters determine how far a point can be to still be included in the model. The method performs generally very well, but in the close vicinity of the scanner, some points are lost. These are typically peak points of small ripples 3-10 mm in size. Some of these were returned to the snow surface by searching for points less than 2 cm above the snow surface with 10 cm maximum triangle edge lengths.

After extracting the snow surface, the surface roughness was calculated. It was done by first selecting a resolution and radius for the areas for which the method is applied. Then a plane is fitted to each resolution unit center, and minimum distance from the plane is calculated for each point less than the predefined radius from the center point. The minimum distance from the plane is determined similarly to the plate profile method so that the roughness is defined as the mean minimum distance of the points to the plane. A sample of the MLS grid roughness data is shown in Figure 16.

The results from the MLS grid method were compared to the plate profiles. The MLS grid test data had 1-meter grid sampling. The sample diameters were from 10 cm to 100 cm in 10 cm intervals. The sample points closest to the plate profiles were used for the comparison. The rms height data of both the methods can be seen in Figure 17. The figure shows that the increase in sample size increases the rms height value of the MLS grid data, as was expected. The largest increase was found for the sites with the largest variation in surface topography. The 10 cm scale turned out to be the most challenging one for MLS grid, which can be explained by the number of points within this area being quite low,

thus causing statistical uncertainty. The low number of points can also affect the accuracy of the plane fitting. This can be helped by measuring denser point clouds in the future.

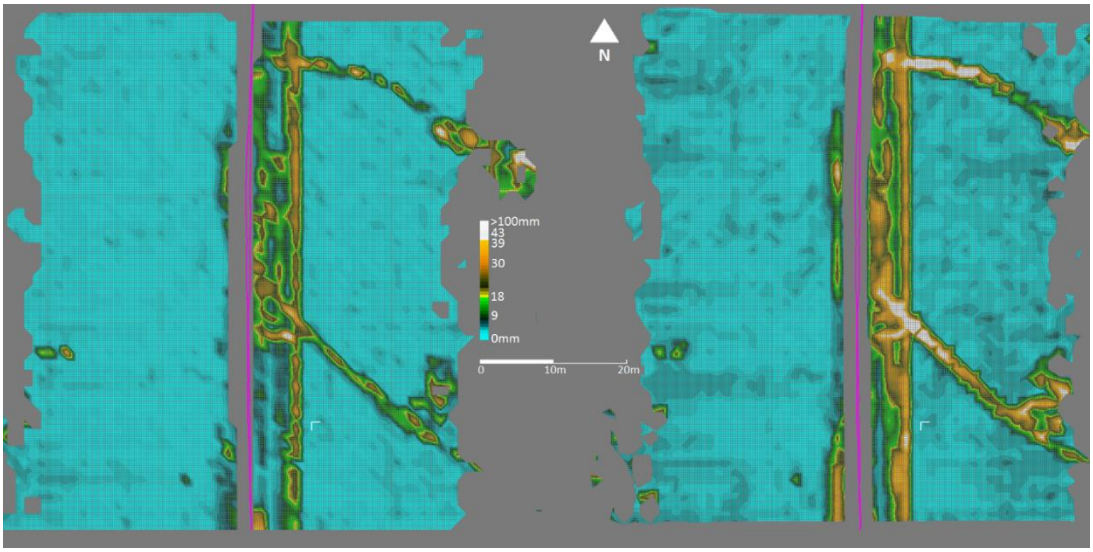

Figure 16 Snow surface roughness from MLS data with 10 cm (left) and 100 cm (right) sample diameters at 1 m grid.

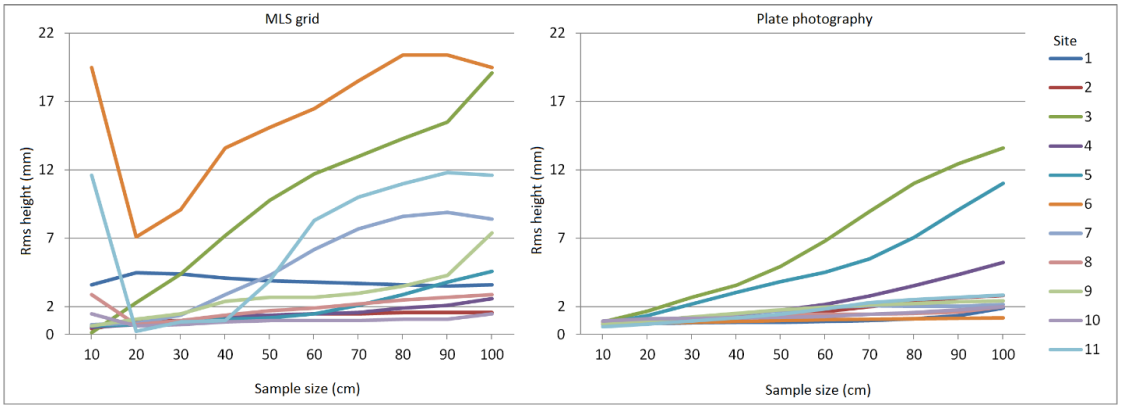

Figure 17 The rms height variation of the snow surface derived by validation plate profiles and MLS grid 3D.

Based on the results the MLS grid method and MLS data show great potential for surface roughness mapping, especially at above centimeter scales. The MLS data can be used to cover large areas, which is particularly useful for satellite data validation and for studying the variability of the snow surface in different environments, such as forested vs open areas.

5. THE ALBEDO OF THE AREAS COVERED BY SEASONAL SNOW

Due to the importance of seasonal snow and surface albedo to the climate, it is important to study them at a global scale. This means vast and remote areas. The in-situ ground measurements do not have sufficient spatial coverage to provide the means to do this, but satellite remote sensing data covers large areas and is available for several decades.

The changes in the albedo of snow covered areas can be studied using satellite-based snow and albedo products. The products use the microwave and/or optical instruments, which are sensitive to the brightness of the surface at measured wavelengths. The optical instruments have typically a higher spatial resolution than the microwave instruments, and can detect even thin snow covers or surface hoar. Therefore they provide data suitable for mapping the snow cover extent, fraction of snow cover and surface albedo. The microwave instruments in turn are more sensitive to the liquid water at and near the surface. This makes microwave instruments good at measuring properties like snow water equivalent, which is a key parameter for hydrological applications such as flood predictions. Furthermore, microwave measurements are typically not sensitive to cloud cover, which prohibits observations of the earth´s surface from the optical sensors.

Currently, there are several snow cover and albedo products available, some of which are more observations-based and some incorporate modeling in the retrieval algorithms (Schaaf et al. 2002, Siljamo & Hyvärinen 2011, Barlage et al. 2015, Riggs & Hall 2015, Anttila et al. 2016). The products can be further divided into operational products designed for snow cover and albedo monitoring, and time series, which are meant for climate studies. The operational products are meant for climate and hydrological monitoring, and weather and flood prediction. They are produced at regular intervals, for example, weekly, biweekly or monthly. The long data records of intercalibrated satellite data form the basis of longer time series, giving means to study long-term climatological changes in snow cover and surface albedo. The surface albedo products can also be used to observe changes in the snow cover, as is done in paper V.

Deriving broadband surface albedo from satellite radiance observations requires several steps. First, the satellite instruments make observations above the atmosphere. If this data is used to derive the albedo of the earth surface, then the observations from clouds also need to be removed and the effect of the atmosphere, both downwards and upwards, needs to be taken into account. Second, the earth surface itself has many different types of land surfaces, which all have different scattering properties (BRDF). Since the satellites measure the reflectance at only one direction, the BRDF is needed to describe the scattering in all other directions to derive the hemispherical reflectance

needed for the surface albedo derivation. Third, satellites observe radiance at a limited number of wavelengths. If the data is used for deriving broadband albedo, then the spectral albedos of the observed wavelengths need to be converted into broadband albedo.

The surface albedo of the snow covered areas consists of reflectance from both the snow cover and the vegetation. Furthermore, the snow conditions vary both spatially and temporally. For instance, the reflective properties are different for different snow surfaces, the trees can be covered by snow or be totally snow free, the fraction of the ground covered by snow can be anything from 0% to 100%, and the snow surface can be either clean or dirty. Thus, it is easy to understand why describing the surface albedo of snow-covered surfaces in the climate models is particularly difficult for the vegetated areas, such as the boreal forest zone. (Essery 2013, Thackeray et al. 2015, Abe et al. 2017). Given the large area covered by the boreal forest, and the large variation in albedo values for this area, more information is needed on the phenomena affecting the albedo and snow cover of this area.

The previous studies have already observed changes in the snow cover and vegetation, which have affected the surface albedo over snow covered areas of the Northern Hemisphere (Hall 2004, Smith et al. 2004, Derý & Brown 2007, Trenberth et al. 2007, Brown & Robinson 2011, Flanner et al. 2011, Derksen & Brown 2012, Foster et al. 2013, Stocker 2014, Atlaskina et al. 2015, Fassnacht et al 2016). The studies on snow cover have focused on the changes in snow cover extent, which has been observed to be decreasing, especially in the spring (Derý & Brown 2007, Brown & Robinson 2011, Derksen & Brown 2012). This has an effect on the springtime albedo during the melt season (Atlaskina et al. 2015). Also, the timing of the melt season has changed, with different trends for different areas (Markus 2009, Wang et al. 2013; Chen et al. 2015, Malnes et al. 2016).

5.1. CHANGES IN SURFACE ALBEDO PRIOR TO MELT IN AREAS COVERED BY SEASONAL SNOW

The changes in albedo and SCE during the melt season have been well reported, but there is very little information on the possible changes in surface albedo prior to the melt season. The study presented here utilizes global albedo data to define the start and end of the melt season, and to look at the albedo level at the start of the melt season to see if there have been changes in surface albedo already before the melt. The albedo levels are derived from the exact time of the start and end of melt.

5.1.1. Methods for retrieving melt season timing and albedo

The melt season parameters are derived from sigmoid fittings of yearly surface albedo data of the 34 years long CLARA-A2 SAL (the Satellite Application Facility for Climate Monitoring (CM SAF, funded by EUMETSAT) CLouds, Albedo and RAdiation second release Surface ALbedo data record (Anttila et al. 2016, Karlsson et al. 2017)) data record. The albedo values of CLARA-A2 SAL are derived from optical satellite data (AVHRR instruments onboard the NOAA and MetOp satellites). The final albedo data used here consists of pentad mean values of black-sky surface albedo corresponding to the wavelengths 0.25 - 2.5 µm. The data is given in 0.25° resolution and covers the years from 1982 to 2015.

The sigmoids fittings are done to each pixel and each year using nonlinear regression (Böttcher et al. 2014) (Figure 18). Only pentads from the end of January until end of August were used. The date of snowmelt onset was defined to be the date at which the sigmoid reached 99 % of its variation range. The corresponding threshold for the end date of the snow melt season was defined to be 1%. The length of the melt season was the time difference between the start and end date of the melt season. The albedo values at the time of the onset and end of melt were used as to represent the albedo values preceding and following the melt season.

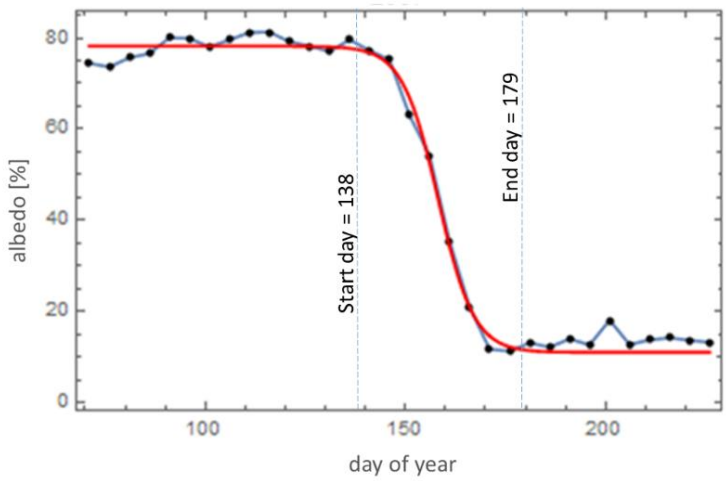

Figure 18 An example of the sigmoid fitting for location 68.125°N, 120.125°E for the year 2007.

The final analysis included only the pixels for which at least 10 years of data were available, the difference between the albedo values at the end and start of melt was larger than 5 % absolute albedo units, and both start and end day of melt were derived successfully. The mean values of R^2 and root mean square error (RMSE) of the final

sigmoid regressions were 0.989 and 5.55 (albedo percentage), respectively. The analysis was made by using only the pixels for which R^2>0.95 and RMSE<20. This resulted in discarding about 2 % of the data. The final dataset consisted of 2.46 million pixel level melt seasons.

The trends for the melt season parameters were determined per pixel over the 34 years using linear regression of rolling five year means. 5-year mean values with fewer than 3 observations were excluded from the analysis. The linear fitting was carried out only for the pixels that had at least 20 mean values. In the end, trends for 72092 pixels were retrieved successfully.

5.1.2. Trends in surface albedo prior to melt

The trends in the albedo at the start of melt season show large spatial variation (Figure 19). The areas of increasing and decreasing albedo values appear in large homogeneous areas typically in the boreal forest zone. Most of the tundra areas do not have statistically reliable (R2>0.5 for the trend fitting) trends. This can be seen in Figure 19b, which shows the land use classes from GlobCover2009 (Arino et al. 2010) for the areas with observed reliable trends in albedo prior to melting. The GlobCover2009 classes are listed in Table 4. In North America, the trends are more scattered when it comes to the direction of change than they are in Eurasia. This fractured nature of the direction of change may be caused by man-made changes in land use types and surface properties, such as cultivation and forestry.

The surface albedo observations prior to melt onset are based on satellite observations. Therefore the albedo values include signal from all land use types at the measured area. The potential effect of vegetation on the observed changes can be estimated by looking at the changes in surface albedo after melt season (Figure 20). These are changes in surface reflectance after the snow has disappeared and before the vegetation has started greening. The albedo after melt shows large areas of homogenous change. The changes are weaker than for albedo prior to melt, as can be expected. The spatial patterns of the post-melt albedo again have similarities with the pre-melt albedo trends suggesting that the causes for the change in winter albedo are related to what is causing the changes in the albedo after melt, but only in some areas. The southern edge of tundra shows weak decreasing trends for the albedo both before and after melt, which could be explained by the shrubification of tundra (Sturm et al. 2001, 2005, Tape et al. 2006, Myers et al. 2011, Pearson et al. 2013, Domine et al. 2016). In northern tundra there are no observed changes, expect for some areas near the northern coast of Eurasia, which show increasing trends. These areas correspond roughly with the areas of increased accumulated precipitation prior to melt, which can be seen in Figure 7 of paper V. In the eastern parts of the Eurasian boreal forest zone the albedo after melt season has decreased. This is also the case in North America in Southern Alaska, Canadian Rocky Mountains, most of

Labrador Peninsula and the northern islands of the Canadian Archipelago. These changes could be explained by larger trees.

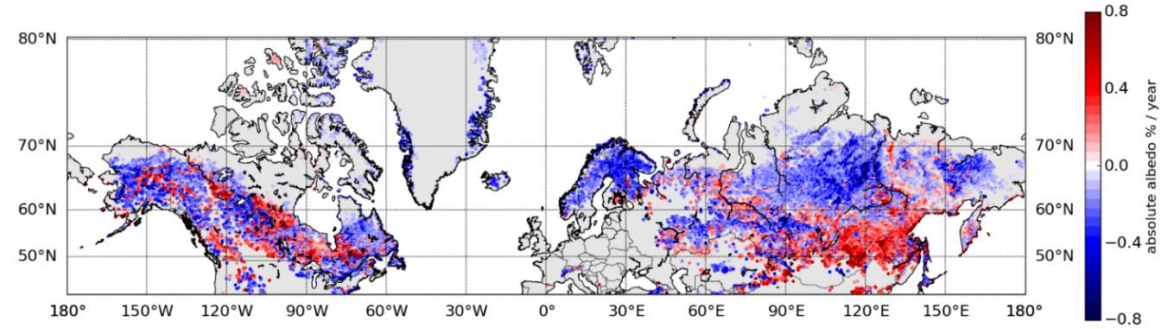

(a)

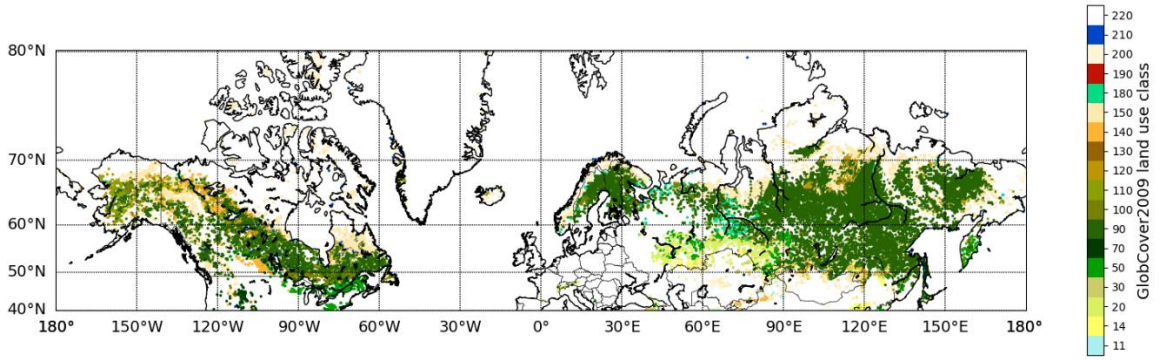

(b)

Figure 19 a) The rate of change in albedo at the start of melt (absolute albedo percentage) over 1982 to 2015. The figure shows cases for which the R^2 for the trend fitting was larger than 0.5. b) The GlobCover2009 land use classes of the pixels with reliable albedo trends.

The role of climate change in the changes observed in pre-melt albedo were studied by using the ERA-Interim re-analysis data (Dee et al. 2011) on wind speed (10 m height), total precipitation, amount of snowfall, air temperature (2 m height) and number of days when the maximum air temperature was above 0°C, 4°C and 10°C degrees. The parameters were studied using the 14 day mean values prior to the onset of melt. The correlation between the climatic parameters and the albedo before melt is shown in Figure 21. Explaining the change in albedo before the onset of melt required six climatic parameters (all except snowfall) derived from ERA-Interim, giving a mean R^2 value for the whole area to be 0.64. The climatic parameters were best at explaining the observed change in pre-melt albedo in Northern China, Scandinavia, and parts of Canadian Archipelago.

Also other factors may have affected the surface albedo. The optical properties of the snow cover (mostly grain size and shape and surface roughness) may have changed due to the large-scale changes in climate (Wiscombe & Warren 1980, Domine et al. 2006). The existing studies show changes in vegetation, permafrost and impurities on snow, all of which can have an effect on surface albedo (Rigina 2002, Smith et al. 2004, Dumont et al. 2009, Piao et al. 2011, Ménédgoz et al. 2013, Xu et al. 2013, Buitenwerf et al. 2015, Bullard et al. 2016, Helbig et al. 2016). The changes in these show similar patterns as the changes in pre-melt surface albedo, but these similarities are not consistent throughout the study area. This could mean that the changes in them are related to the changes observed on albedo, but the dominating cause for the changes in albedo is different for different areas. It is also noteworthy that the effect of these changes on surface albedo is not the same in all areas.

Table 4 GlobCover2009 classes and the number of occurrences they were found to be the most common land use class in the area of one SAL pixel.

LUC class	Label	number of occurrences
11	Post-flooding or irrigated croplands (or aquatic)	420
14	Rainfed croplands	5137
20	Mosaic cropland (50-70%) / vegetation (grassland/shrubland/forest) (20-50%)	5771
30	Mosaic vegetation (grassland/shrubland/forest) (50-70%) / cropland (20-50%)	2996
50	Closed (>40%) broadleaved deciduous forest (>5m)	7775
70	Closed (>40%) needleleaved evergreen forest (>5m)	2472
90	Open (15-40%) needleleaved deciduous or evergreen forest (>5m)	31415
100	Closed to open (>15%) mixed broadleaved and needleleaved forest (>5m)	3605
110	Mosaic forest or shrubland (50-70%) / grassland (20-50%)	2299
120	Mosaic grassland (50-70%) / forest or shrubland (20-50%)	1883
130	Closed to open (>15%) (broadleaved or needleleaved, evergreen or deciduous) shrubland (<5m)	1371
140	Closed to open (>15%) herbaceous vegetation (grassland, savannas or lichens/mosses)	3869
150	Sparse (<15%) vegetation	28741
180	Closed to open (>15%) grassland or woody vegetation on regularly flooded or waterlogged soil - Fresh, brackish or saline water	1639
190	Artificial surfaces and associated areas (Urban areas >50%)	103
200	Bare areas	7523
210	Water bodies	115239
220	Permanent snow and ice	11022

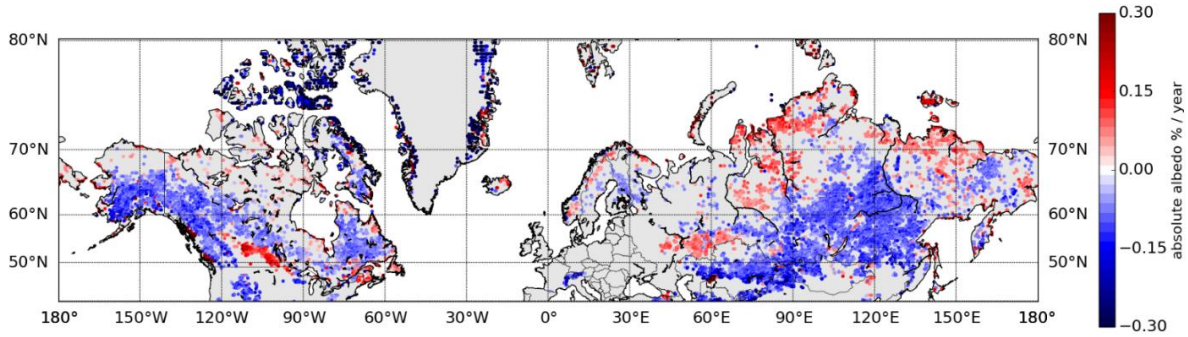

Figure 20 The rate of change in albedo at the end of melt (absolute albedo percentage) from 1982 to 2015. The figure shows cases for which the R^2 for the trend fitting was larger than 0.5. The negative values mean decreasing albedo and the positive values mean increasing albedo.

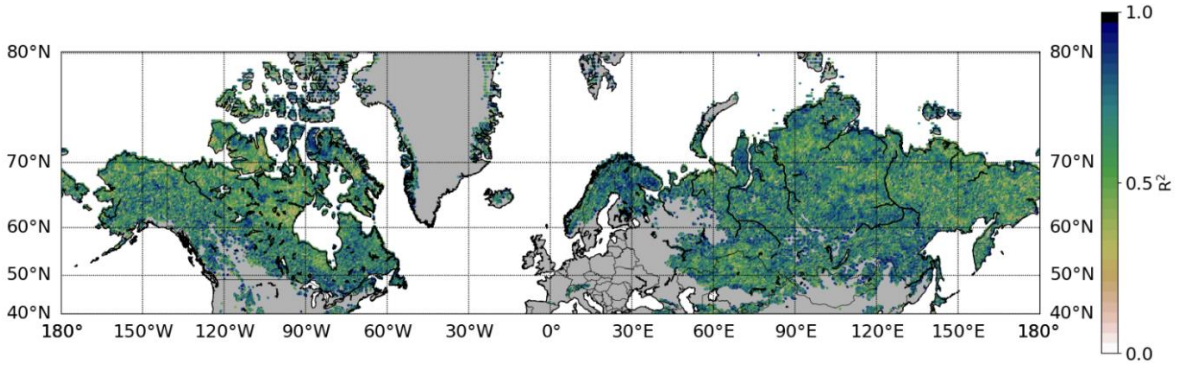

Figure 21 The correlation (R^2) between the albedo before the onset of melt and 6 climatic parameters derived from ERA-Interim climate data for 14 days prior to melting. The climatic parameters were the mean air temperature, mean wind speed, total precipitation and the number of days when the air temperature was above 0°C, 4°C and 10°C degrees.

5.1.3. Trends in melt season timing

The statistically reliable (R^2>0.5) changes in melt season timing also concentrate on larger homogeneous areas (Figure 22). The changes are significant, but the direction of change varies within the study area. The majority of the observations show no clear trends. The trends do not seem to be as strongly linked to the vegetation type as the pre-melt albedo. For example, the whole of Central Siberian Plain shows trends towards earlier onset and end of melt, with the length of melt season remaining the same, even though the area includes both boreal forest and tundra. Most of the observed clear trends were towards longer melt seasons and earlier onset of melt, as was the case with Northern Canadian Rocky Mountains and Northern China and Mongolia. As with albedo, in North America the trends are typically more scattered than in Eurasia showing small-scale spatial variation.

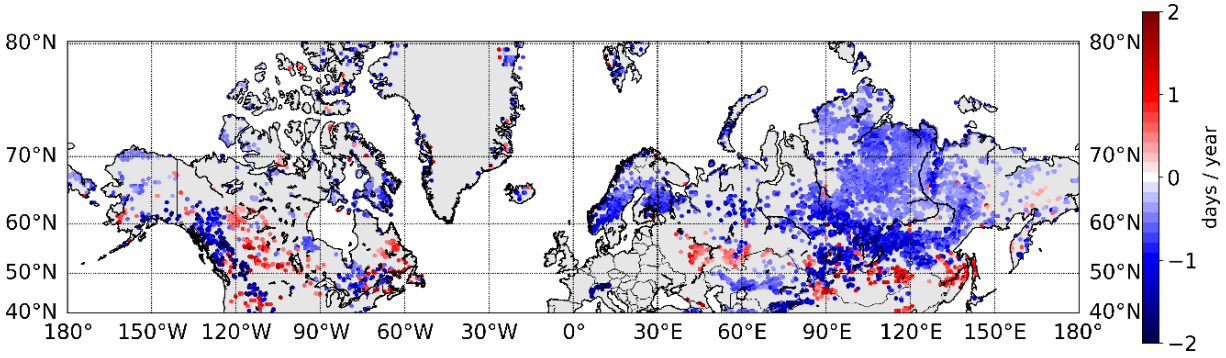

(a)

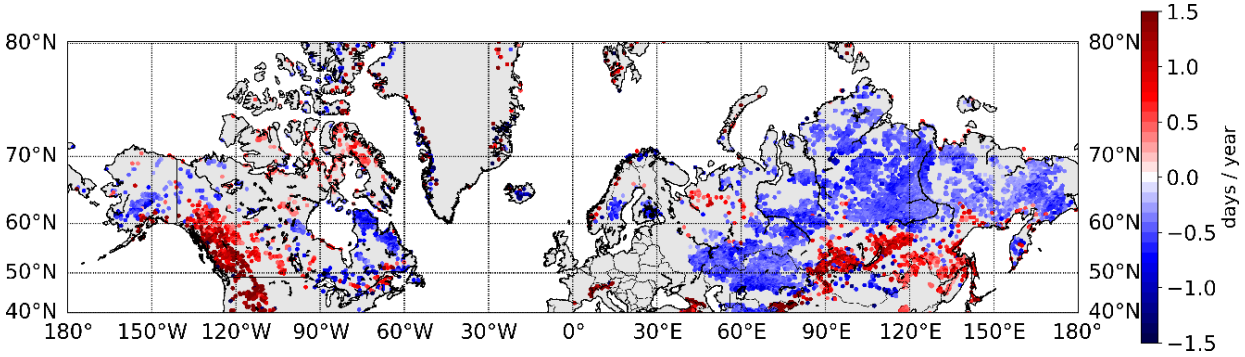

(b)

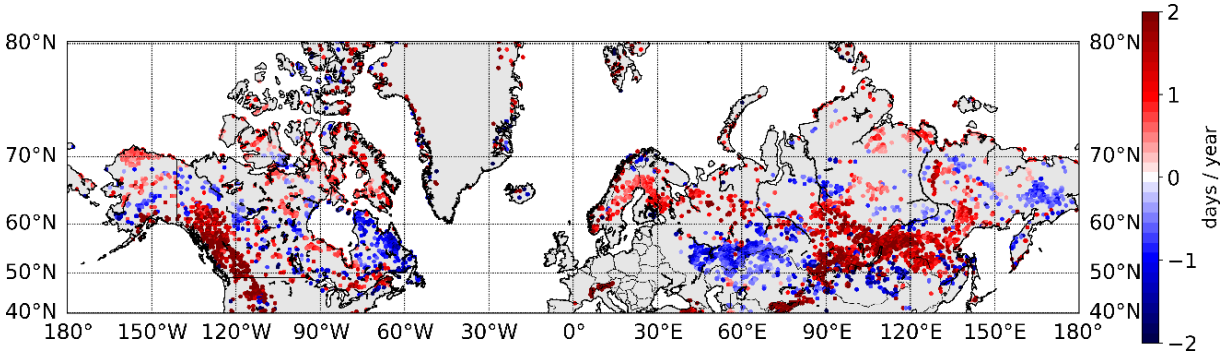

(c)

Figure 22 a) The rates of change for the start day of melt between 1982 and 2015 showing cases for which R^2 of the fit was larger than 0.5. The negative values mean earlier onset of melt and the positive values mean later dates of onset of melt. b) The rates of change for the end day of melt between 1982 and 2015 using 5-year rolling mean albedo (showing cases for which R^2 of the fit was larger than 0.5). The negative values mean the earlier end of melt and the positive values mean later dates of end of melt. c) The rates of change for the length of the melt season between 1982 and 2015 (showing cases for which R^2 of the fit was larger than 0.5). The negative values mean shorter melt seasons and the positive values mean longer melt seasons.

Looking at the correlation between the start day of melt and climate, three parameters were enough to explain the observed change, with the R^2 value being 0.65 (Figure 23). The climatic parameters used were mean air temperature, mean wind speed, and

accumulated precipitation. The observed changes in start day of melt season were best explained by the climatic parameters in Northern China and Mongolia, where the climatic parameters were able to explain the change almost completely. The parameter best explaining the change was the mean air temperature (mean R^2=0.51 for the whole area), but the climatic parameter best explaining the change was different in different areas.

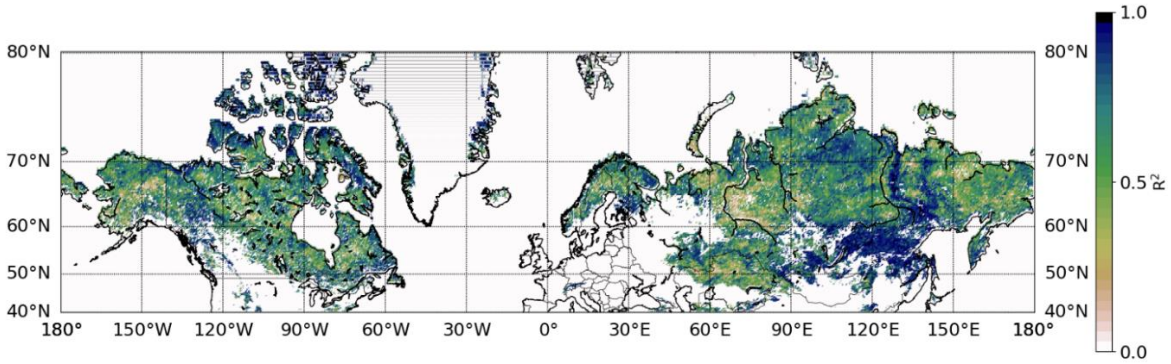

Figure 23 The correlation (R^2) between the start day of melt and 3 climatic parameters derived from ERA-Interim climate data for 14 days prior to melting. The climatic parameters used here were mean air temperature, mean wind speed, and accumulated precipitation.

The albedo prior to melt season of Northern Hemisphere land areas with seasonal snow cover has changed over the period 1982 to 2015. The direction of change depends on the area. Also the timing of melt season has changed over the same time period. These changes vary between different areas. The changes in albedo prior to melt are linked to changes in vegetation, whereas the changes in melt season timing are linked to changes in climatic conditions. More research is needed to study the local drivers for the observed changes.

6. CONCLUSIONS

The brightness of seasonal snow affects the climate and global energy budget. The reflective properties of seasonal snow are also important parameters for remote sensing and climate models. This dissertation has contributed to the understanding of snow optical properties and improved the usability of remote sensing data (both optical satellite data and laser scanning data) on snow-covered surfaces.

The main contributions of this dissertation have been:

- Currently, there are no standardized methods to measure snow surface roughness as it is difficult to measure. Here, new methods have been created, validated and tested.
    - The plate photography based method for measuring snow surface roughness has been validated and the method has been used in the field. It has proven to be easy and reliable also in field conditions.
    - The mobile laser scanning based method for measuring sow surface roughness has been validated against plate profiles and the mobile laser scanning data has been shown to be suitable for mapping the height variation of the snow surface.
- The surface roughness of natural snow depends on the measured scale. Therefore the surface features should be described using parameters that cover all necessary scales.
    - The multiscale parameters describing snow surface roughness have been used on an extensive field data set of plate photography –profiles. They have been shown to describe the regularity of the surface features as well as the magnitude of the height variation. They are also able to distinguish between old and fresh snow.
- Validating satellite remote sensing data on snow cover needs validation data that includes information from larger areas instead of pointwise measurements. In this dissertation, the usability of terrestrial laser scanning data has been improved by studying the behavior of laser backscatter on different snow surfaces.
    - The depth of the backscatter of the laser beam has been shown to take place at the very surface.
    - The incidence angle dependency of the intensity of the backscattering of laser scanning data does not depend on the surface crystal type. Therefore in the future, the backscattering intensity data can be used for snow cover classifications and snow brightness studies.

- Long-term changes in the surface brightness of snow-covered areas need to be studied on a global scale. Here the remote sensing data on surface albedo has been used to study the changes in surface albedo on snow-covered areas.
    - The changes in surface albedo of snow-covered surfaces prior to melt season in Northern Hemisphere land areas between 40°N and 80°N have been investigated. The reliable trends seem to concentrate on the boreal forest zone. The pre-melt albedo of the tundra area has not yet experienced noticeable change.
    - The timing of the melt season in Northern Hemisphere land areas between 40°N and 80°N has changed in particular in the Central Siberian Plane, where the melt season takes place earlier, and in Northern China and Mongolia, and Canadian Archipelago, where the melt season starts earlier, ends later, and lasts for longer. The changes are related to climatic factors.

During the writing of this dissertation, the work on studying small scale roughness is taking first steps with methods and parameters being developed by several groups of researches around the world. The importance of small scale surface roughness on the optical properties of snow has been recognized by the international community, but very little has been done on studying it in detail. Typically the studies cover only a few profiles and snow types, and the parameters that are used vary from study to study. The multiscale nature of the phenomenon is recognized by some, but the directionality is still largely left without notice.

Today, 10 years after the SNORTEX -campaign, the plate-photography data set of surface roughness profiles and supporting geophysical measurements is still the largest data set on the surface roughness of natural snow cover that is available, covering several different snow cover types. After the development of the methods to measure surface roughness presented in this dissertation, new methods have been created, but they are mostly used for medium and large scale roughness.

Laser scanning has become a standard measurement technique for snow depth and is used in an increased number of operational measuring sites. The applications on snow surfaces that use the backscattering intensity are few, but show great potential. The intensity information of the backscattering of the laser beam provides means to study the reflectance of snow surface in one direction. As new methods are being developed, this data could in the future be used to study the hemispherical reflectance of the snow surface.

The global climate change, greening and browning of Boreal Forests and tundra and the changes in surface albedo, vegetation and permafrost is an area of study that is progressing with huge steps. Papers on this are published on a weekly basis. The research on the changes in albedo of areas with seasonal snow have focused on monthly means and melt season. The data and results presented in this dissertation define the exact timing of the melt season and thus enable more detailed studies on the changes in surface

albedo of areas with seasonal snow. The results have risen large interest in particular amongst the modelling community, and there is currently co-operation with several different modelling and reanalysis groups.

In the future, the surface roughness data set should be accompanied with other similar data sets from different areas of the world to globally cover the different snow types. The plate methods could be adapted to use a smaller plate that could be used for measuring surface roughness in even smaller scales. Together, the plate-photography -based methods and the MLS method could be used to incorporate information on surface roughness in a larger range of scales, from crystal scale to kilometer scale. The methods could be used to gather data on a larger variety of snow types around the globe. This information could be used to combine the two surface roughness parameters into one and to develop more accurate scattering descriptions of seasonal snow.

The role of surface roughness on reflectance not only on single directions, but hemispherical reflectance (surface albedo) should be studied further. The large variation of snow types and surface features, combined with all the factors influencing surface albedo makes the relationship between surface roughness and albedo a very complex entity. The increasing amount of data on surface roughness and albedo will help to progress this work in the future.

The changes in pre-melt surface albedo of snow-covered areas should be studied further to investigate the role of vegetation and land use type in more detail, perhaps using also stem height and forest density information. The change in albedo and melt season timing could be studied in more detail to describe the variability of change during the 34 years. The results could be used to look in more detail on the local drivers of the observed changes.

These results improve the possibility to gather and analyze snow surface roughness information also from vast, remote and potentially dangerous areas. The improved understanding of seasonal snow surface roughness and albedo will contribute to the accuracy of climate models and remote sensing data. The improved parameterization of seasonal snow surface roughness gives means to incorporate the knowledge on surface roughness to scattering models of snow. This will contribute to the accuracy of remote sensing based surface albedo products, which can serve as validation data for climate models and input parameters for reanalysis data. The understanding of the changes in surface albedo for the last decades improves our understanding of the changing climate and the effect it has on the snow-covered areas.

REFERENCES

Abe, M., Takata, K., Kawamiya, M., & Watanabe, S. (2017). Vegetation masking effect on future warming and snow albedo feedback in a boreal forest region of northern Eurasia according to MIROC-ESM. *Journal of Geophysical Research: Atmospheres, 122,* doi:10.1002/2017JD026957.

Ahokas, E., Kaasalainen, S., Hyyppä, J., & Suomalainen, J. (2006). Calibration of the Optech ALTM 3100 laser scanner intensity data using brightness targets. *Int. Arch. Photogramm. Remote. Sens. Spat. Inf. Sci.*, *34*, 3-6.

Anttila, K., Kaasalainen, S., Krooks, A., Kaartinen, H., Kukko, A., Manninen, T., Lahtinen, P., & Siljamo, N. (2011). Radiometric calibration of TLS intensity: Application to snow cover change detection. *Int. Arch. Photogramm. Remote. Sens. Spat. Inf. Sci.*, *38* (5 / W12).

Anttila, K., Jääskeläinen, E., Riihelä, A., Manninen, T., Andersson, K., & Hollman, R. (2016). Algorithm Theoretical Basis Document: CM SAF Cloud, Albedo, Radiation data record ed. 2 – Surface Albedo. Doi: 10.5676/EUM_SAF_CM/CLARA_AVHRR/V002 (2016).

Atlaskina, K., Berninger, F. & Leeuw, G. (2015). Satellite observations of changes in snow-covered land surface albedo during spring in the Northern Hemisphere. *The Cryosphere, 9,* 1879-1893.

Arino, O., J. Ramos, V. Kalogirou, P. Defourny, & F. Achard, 2010: GlobCover 2009. *Proceedings of the living planet Symposium*, SP-686, June 2010.

Armstrong, R.L. & Brun E., ed. (2008). Snow and climate, Cambridge University Press, New York.

Arnold, N. S., Rees, W. G., Devereux, B. J., & Amable, G. S. (2006). Evaluating the potential of high-resolution airborne LIDAR data in glaciology. *International Journal of Remote Sensing*, *27*(6), 1233-1251.

Axelsson, P. (1999). Processing of laser scanner data — algorithms and applications. *ISPRS Journal of Photogrammetry and Remote Sensing*, *54*(2–3), 138–147.

Barlage, M., Zeng, X., Wei, H., & Mitchell, K. E. (2005). A global 0.05˚ maximum albedo dataset of snow-covered land based on MODIS observations. *Geophysical Research Letters, 32,* L17405, doi: 10.1029/2005GL022881.

Böttcher, K., Aurela, M., Kervinen, M., Markkanen, T., Mattila, O.-P., Kolari, P.,… & Pulliainen, J. (2014). MODIS tile-series-derived indicators for the beginning of the growing season in boreal coniferous forest – A comparison with the CO_2 flux measurements and phenological observations in Finland. *Remote Sensing of Environment, 140,* 625-638.

Brown, R.D., & Mote, P.W. (2009). The response of Northern Hemisphere snow cover to a changing climate. *Journal of Climate*, *22*, 2124-2144.

Brown, R.D., & Robinson, D.A. (2011). Northern Hemisphere spring snow cover variability and change over 1922– 2010 including an assessment of uncertainty. *The Cryosphere, 5*, 219-229, doi:10.5194/tc-5-219-2011.

Budyko, M. I. (1969). The effect of solar radiation variations on the climate of the earth. *tellus*, *21*(5), 611-619.

Buitenwerf, R., Rose, L., & Higgins, S. (2015). Three decades of multi-dimensional change in global leaf phenology. *Nature Climate Change, 5,* 364-368.

Bullard, J., Baddock, M., Bradwell, T., Crusius, J., Darlington, E., Gaiero, D., … & Thorsteinsson, T. (2016). High-latitude dust in Earth system. *Reviews on Geophysics, 54,* 447–485, doi:10.1002/2016RG000518.

Chen, X., Liang, S., Cao, Y., Cao, T., & Wang, D. (2015). Observed contrast changes in snow cover phenology in northern middle and high latitudes from 2001-2014. *Science Reports, 5,* doi: 10.1038/srep16820.

Choi, G., Robinson, D.A., & Kang, S. (2010). Changing Northern Hemisphere snow seasons. *Journal of Climate*, *23*, 5305-5310.

Choudhury, B. J., & Chang, A. T. C. (1981). The albedo of snow for partially cloudy skies. *Boundary-Layer Meteorology*, *20*(3), 371-389.

Church, E. L. (1988). Fractal surface finish. *Appl. Opt.*, *27*(89), 1518–1526.

Colbeck, S.C. (1982a). An overview of seasonal snow metamorphism. *Reviews of Geophysics and Space Physics*, *20*(1), 45-61.

Colbeck, S.C. (1982b). Growth of faceted crystals in a snow cover. CRREL Report 82-29. 27 pp.

Colbeck, S. C. (1997). *A Review of Sintering in Seasonal Snow* (No. CRREL-97-10). COLD REGIONS RESEARCH AND ENGINEERING LAB HANOVER NH.

Coren, F., & Sterzai, P. (2006). Radiometric correction in laser scanning. *International Journal of Remote Sensing, 27*, 3097-3104.

Davidson, M., Le Toan, T., Mattia, F., Manninen, T., & Borgeaud, M. (2000). On the characterisation of agricultural random roughness for radar remote sensing studies. *IEEE Transactions on Geoscience and Remote Sensing*, *38*(2), 630–640.

Dee, D. P., Uppala, S. M., Simmons, A. J., Berrisford, P., Poli, P., Kobayashi, S., ... & Bechtold, P. (2011). The ERA-Interim reanalysis: Configuration and performance of the data assimilation system. *Quarterly Journal of the royal meteorological society*, *137*(656), 553-597.

Deems, J. S., Fassnacht, S. R., & Elder, K. J. (2006). Fractal distribution of snow depth from LiDAR data. *Journal of Hydrometeorology*, *7*(2), 285-297.

Derksen, C., & Brown, R. (2012). Spring snow cover extent reductions in the 2008–2012 period exceeding climate model predictions. *Geophysical Research Letters, 39*, L19504.

Déry, S., & Brown, R. (2007). Recent Northern Hemisphere snow cover extent trends and implications for the snow-albedo feedback. *Geophysical Research Letters, 34,* L22504.

Domine, F., Salvatori, R., Legagneux, L., Salzano, R., Fily, M., & Casacchia, R. (2006). Correlation between the specific surface area and the short wave infrared (SWIR) reflectance of snow. *Cold Regions Science and Technology, 46*(1)*,* 60–68.

Domine, F., Barrere, M., & Morin, S. (2016). The growth of shrubs on high Arctic tundra at Bylot Island: impact on snow physical properties and permafrost thermal regime. *Biogeosciences*, *13*(23), 6471.

Dong, W. P., Sullivan, P. J., & Stout, K. J. (1992). Comprehensive study of parameters for characterizing three-dimensional surface topography I: Some inherent properties of parameter variation. *Wear*, *159*, 161–171.

Dong, W. P., Sullivan, P. J., & Stout, K. J. (1993). Comprehensive study of parameters for characterizing three-dimensional surface topography II: Statistical properties of parameter variation. *Wear*, *167*, 9–21.

Dong, W. P., Sullivan, P. J., & Stout, K. J. (1994a). Comprehensive study of parameters for characterizing three-dimensional surface topography III: Parameters for characterising amplitude and some functional properties. *Wear*, *178*, 29–43.

Dong, W. P., Sullivan, P. J., & Stout, K. J. (1994b). Comprehensive study of parameters for characterizing three-dimensional surface topography IV: Parameters for characterising spatial and hybrid properties. *Wear*, *178*, 45–60.

Dumont, M., Brun, E., Picard, G., Michou, M., Libois, Q., Petit, J. R., ... & Josse, B. (2014). Contribution of light-absorbing impurities in snow to Greenland's darkening since 2009. *Nature Geoscience*, *7*(7), 509.

Egli, L., Jonas, T., Grünewald, T., Schirmer, M., & Burlando, P. (2012). Dynamics of snow ablation in a small Alpine catchment observed by repeated terrestrial laser scans. *Hydrological Processes*, *26*(10), 1574–1585.

Eitel, J. U. H., Williams, C. J., Vierling, L. A., Al-Hamdan, O. Z., & Pierson, F. B. (2011). Suitability of terrestrial laser scanning for studying surface roughness effects on concentrated flow erosion processes in rangelands. *CATENA 87*(3), 398–407.

Elder, K., Cline, D., Liston, G., & Armstrong, R. (2009). NASA Cold Land Processes Experiment (CLPX 2002/03): Field measurements of snowpack properties and soil moisture. *Journal of Hydrometeorology*, *10*, 320–329.

Essery, R. (2013). Large-scale simulations of snow albedo masking by forests. *Geophysical Research Letters, 40*, doi: 10.1002/grl.51008

Eveland, J. W., Gooseff, M. N., Lampkin, D. J., Barrett J. E., & Takacs-Vesbach, C. D. (2013). Seasonal controls on snow distribution and aerial ablation at the snow patch and landscape scales, McMurdo Dry Valleys, Antarctica. *The Cryosphere*, *7*, 917-913.

Fassnacht, S., Cherry, M., Venable, N., & Saavedra, F. (2016). Snow and albedo climate change impacts across the United States Northern Great Plains. *The Cryosphere*, *10,* 329-339.

Fassnacht, S. R., & Deems, J. D. (2006). Measurement sampling and scaling for deep montane snow depth data. *Hydrological Processes*, *20*, 829–838.

Fassnacht, S. R., Stednick, J. D., Deems, J. S., & Corrao, M. V. (2009a). Metrics for assessing snow surface roughness from digital imagery. *Water Resources Research*, *45*, W00D31, doi:10.1029/2008WR006986.

Fassnacht, S. R., Williams, M. W., & Corrao, M. V. (2009). Changes in the surface roughness of snow from millimetre to metre scales. *Ecological Complexity*, *6*(3), 221-229.

Fierz, C., Armstrong, R.L., Durand, Y., Etchevers, P., Greene, E., McClung, D.M., Nishimura, K., Satyawali, P.K., & Sokratov, S.A. (2009). The International Classification for Seasonal Snow on the Ground. IHP-VII Technical Documents in Hydrology N°83, IACS Contribution N°1, UNESCO-IHP, Paris.

Flanner, M.G., Shell, K.M., Barlage, M., Perovich, D.K., & Tschudi, M.A. (2011). Radiative forcing and albedo feedback from the northern hemisphere cryosphere between 1979 and 2008. *Nature Geosciences*, *4*, 151–155. http://dx.doi.org/10.1038/ngeo1062

Foster, J. L., Cohen, J., Robinson, D. A., & Estilow, T. W. (2013). A look at the date of snowmelt and correlation with the Arctic Oscillation. *Annals of Glaciology, 54,* 196-204.

Fung, A. K. (1994). Microwave Scattering and Emission Models and Their Applications, pp. 573, Artech House, Boston.

Gallet, J. C., Domine, F., Zender, C. S., & Picard, G. (2009). Measurement of the specific surface area of snow using infrared reflectance in an integrating sphere at 1310 and 1550 nm. *The Cryosphere, 3*, 167-182, doi:10.5194/tc-3-167-2009.

Gallet, J. C., Domine, F., & Dumont, M. (2014). Measuring the specific surface area of wet snow using 1310 nm reflectance. *The Cryosphere*, *8*(4), 1139.

GCOS Secretariat (2006). Systematic observation requirements for satellite-based products for climate. Technical Report 107, Global Climate Observing System,World Meteorological Organization, 7 bis, Avenue de la Paix P.O. Box No. 2300 CH-1211 Geneva 2, Switzerland.

Gromke, C., Manes, C., Walter, B., Lehning, M., & Guala, M. (2011). Aerodynamic roughness length of fresh snow. *Boundary Layer Meteorology*, *141*, 21–34.

Hakala, T., Suomalainen, J., Kaasalainen, S., & Chen, Y. (2012). Full Waveform Hyperspectral LiDAR for Terrestrial Laser Scanning. *Optics Express*, *20*(7), 7119-7127. http://dx.doi.org/10.1364/OE.20.007119

Hall, A. (2004). The role of surface albedo feedback in climate. *Journal of Climate, 17*, 1550-1568.

Helbig, M., Wischnewski, K., Kljun, N., Chasmer, L. E., Quinton, W. L., Detto, M., & Sonnentag, O. (2016). Regional atmospheric cooling and wetting effect of permafrost thaw-induced boreal forest loss. *Global Change Biology, 22*(12)*,* 0448-4066.

Helfricht, K., Kuhn, M., Keuschnig, M., & Heilig, A. (2014). Lidar snow cover studies on glaciers in the Ötztal Alps (Austria): comparison with snow depths calculated from GPR measurements. *The Cryosphere*, *8*, 41-57.

Herzfeld, U. C. (2002). Vario functions of higher order—Definition and application to characterization of snow surface roughness. *Computers & geosciences*, *28*(5), 641-660.

Höfle, B., Geist, T., Rutzinger M., & Pfeifer, N. (2007). Glacier surface segmentation using airborne laser scanning point cloud and intensity data, *Proceedings of ISPRS Workshop Laser Scanning SilviLaser*, *36*, pp. 195–200, International Archives of Photogrammetry and Remote Sensing, Espoo, Finland part 3/W52.

Höfle, B., & Pfeifer, N. (2007). Correction of laser scanning intensity data: Data and model-driven approaches. *ISPRS journal of photogrammetry and remote sensing*, *62*(6), 415-433.

Holland, M. M., Serreze, M. C., & Stroeve, J. (2010). The sea ice mass budget of the Arctic and its future change as simulated by coupled climate models. *Climate Dynamics*, *34*(2-3), 185-200.

Hollaus, M., Aubrecht, C., Höfle, B., Steinnocher, K., & Wagner, W. (2011). Roughness mapping on various vertical scales based on full-waveform airborne laser scanning data. *Remote Sensing*, *3*, 503–523.

Hood, J. L., & Hayashi, M. (2010). Assessing the application of a laser rangefinder for determining snow depth in inaccessible alpine terrain. *Hydrology and Earth System Sciences*, *14*(6), 901.

Hori, M., Sugiura, K., Kobayashi, K., Aoki, T., Tanikawa, T., Kuchiki, K., Niwano, M., & Enomoto, H. (2017). A 38-year (1978–2015) Northern Hemisphere daily snow cover extent product derived

using consistent objective criteria from satellite-borne optical sensors. *Remote Sensing of Environment*, *191*, 402–418.

Ingvander, S., Brown, I. A., Jansson, P., Holmlund, P., Johansson, C., & Rosqvist, G. (2013). Particle size sampling and object-oriented image analysis for field investigations of snow particle size, shape, and distribution. *Arctic, antarctic, and alpine research*, *45*(3), 330-341.

Ingvander, S., Johansson, C., Jansson, P., & Pettersson, R. (2012). Comparison of digital and manual methods of snow particle size estimation. *Hydrology Research*, *43*(3), 192-202.

Jaedicke, C., Thiis, T.K., & Bang B. (2000). The snowdrift pattern around a small hill in the Arctic. Snow engineering – recent advances and developments. Proceedings of the Fourth International Conference on Snow Engineering, In File, Trondheim, Norway, Rotterdam, A.A. Balkema 75-80.

Jin, Z., Charlock, T. P., & Rutledge, K. (2002). Analysis of broadband solar radiation and albedo over the ocean surface at COVE. *Journal of Atmospheric and Oceanic Technology*, *19*(10), 1585-1601.

Kaasalainen, S., Kaasalainen, M., Mielonen, T., Suomalainen, J., Peltoniemi, J. I., & Näränen, J. (2006). Optical properties of snow in backscatter. *Journal of Glaciology*, *52*, 574–584.

Kaasalainen, S., Kaartinen, H., & Kukko, A. (2008). Snow cover change detection with laser scanning range and brightness measurements. *EARSeL eProceedings*, *7*, 133–141.

Kaasalainen, S., Hyyppä, H., Kukko, A., Litkey, P., Ahokas, E., Hyyppä, J., Lehner, H., Jaakkola, A., Suomalainen, J., & Akujärvi, A. (2009). Radiometric calibration of LIDAR intensity with commercially available reference targets. IEEE *Transactions on Geoscience and Remote Sensing, 47*, -598.

Kaasalainen, S., Kaartinen, H., Kukko, A., Anttila, K., & Krooks, A. (2010). Brief communication: application of mobile laser scanning in snow cover profiling. *The Cryosphere*, *5*, 135–138.

Kaasalainen, S., Jaakkola, A., Kaasalainen, M., Krooks, A., & Kukko, A. (2011). Analysis of incidence angle and distance effects on terrestrial laser scanner intensity: Search for correction methods. *Remote Sensing*, *3*(10), 2207-2221.

Karlsson, K.-G., Anttila, K., Trentmann, J., Stengel, M., Meirink, J. F., Devasthale, A., ... & Benas, N. (2017). CLARA-A2: the second edition of the CM SAF cloud and radiation data record from 34 years of global AVHRR data. *Atmospheric Chemistry and Physics, 17*(9), 5809-5828.

Keller, J. M., Crownover, R. M., & Chen, R. Y. (1987). Characteristics of natural scenes related to the fractal dimension. *IEEE Transactions on Pattern Analysis and Machine Intelligence*, (5), 621-627.

Kenner, R., Phillips, M., Danioth, C., Denier, C., Thee, P., & Zgraggen, A. (2011). Investigation of rock and ice loss in a recently deglaciated mountain rock wall using terrestrial laser scanning: Gemsstock, Swiss Alps. *Cold Regions Science and Technology, 67*(3), 157–164.

Krooks, A., Kaasalainen, S., Hakala, T., & Nevalainen, O. (2013). Correction of Intensity Incidence Angle Effect in Terrestrial Laser Scanning. *ISPRS Ann. Photogramm. Remote Sens. Spatial Inf. Sci.* II-5/W2, 145-150. www.isprs-ann-photogramm-remote-sens-spatial-inf-sci.net/II-5-W2/145/2013/

Kuchiki, K., Aoki, T., Niwano, M., Motoyoshi, H. & Iwabuchi, H. (2011). Effet of sastrugi on snow bidirectional reflectance and its application to MODIS data. *Journal of Geophysical Research*, *116*(D181101).

Kukko, A., Andrei, C. O., Salminen, V. M., Kaartinen, H., Chen, Y., Rönnholm, P., ... & Kosonen, I. (2007). Road environment mapping system of the Finnish Geodetic Institute—FGI Roamer. *Int. Arch. Photogramm. Remote Sens. Spat. Inf. Sci*, *36*, 241-247.

Kukko, A., Anttila, K., Manninen, T., Kaartinen, H., & Kaasalainen, S. (2013). Snow surface roughness from mobile laser scanning data. *Cold Regions Science and Technology*, *96*, 23–35.

Lacroix, P., Legrésy, B., Langley, K., Hamran, S. E., Kohler, J., Roques, S., Rémy, F., & Dechambre, M. (2008). Instruments and methods: In situ measurements of snow surface roughness using a laser profiler. *Journal of Glaciology*, *54*(187), 753–762.

Lamb, D., & Verlinde, J. (2011). *Physics and chemistry of clouds*. Cambridge University Press.

Lehning, M., Löwe, H., Ryser, M., & Raderschall, N. (2008). Inhomogeneous precipitation distribution and snow transport in steep terrain. *Water Resources Research*, *44*, W07404, doi:10.1029/2007WR006545.

Lehning, M., Grünewald, T., & Schirmer, M. (2011). Mountain snow distribution governed by an altitudinal gradient and terrain roughness. *Geophysical Research Letters*, *38*, L19504, doi:10.1029/2011GL048927.

Leroux, C. &Fily, M. (1998). Modeling the effect of sastrugi on snow reflectance. *Journal of Geophysical Research*, *103*(E11).Libbrecht, K. G. (2005). The physics of snow crystals. *Reports on progress in physics*, *68*(4), 855.

Löwe, H., Egli, S., Bartlett, S., Guala, J.M.M., & Manes, C. (2007). On the evolution of the snow surface during snowfall. *Geophysical Research Letters*, *34*, L21507.

Lutz, E. R., Geist, T., & Stötter, J. (2003). Investigations of Airborne Laser Scanning Signal Intensity on glacial surfaces: utilizing comprehensive Laser Geometry Modeling and Surface Type Modeling; (a case study: Svartisheibreen, Norway). *Int. Arch. Photogramm. Remote. Sens. Spat. Inf. Sci.*, *34* (3/W13).

Magono, C., & Chung, W. (1966). Meteorological classification of natural snow crystals. *Journal of the Faculty of Science, Hokkaido University. Series 7, Geophysics*, *2*(4), 321-335.

Makkonen, L. (1989). Estimation of wet snow accretion on structures. *Cold Regions Science and Technology*, *17*(1), 83-88.

Malnes, E., Karlsen, R. S., Johansen, B., Bjerke, J. W., & Tømmervik, H. (2016). Snow season variability in a boreal-Arctic transition area monitored by MODIS data. *Environmental Research Letters, 11*(12), 125005.

Manes, C., Guala, M., Löwe, H., Bartlett, S., Egli, L., & Lehning, M. (2008). Statistical properties of fresh snow roughness. *Water Resources Research*, *44*, W11407, doi:10.1029/2007WR006689.

Manninen, A. T. (1997a). Multiscale surface roughness and backscattering. *Prog. Electromagnet. Res. PIER*, *16*, 175–203.

Manninen, A. T. (1997b). Surface roughness of Baltic sea ice. *Journal of Geophysical Research*, *102*(C1), 1119–1139, doi:10.1029/96JC02991.

Manninen, A. T. (2003). Multiscale surface roughness description for scattering modeling of bare soil. *Physica A*, *319*, 535–551.

Manninen, T., & Roujean, J. L. (2014). SNORTEX field campaigns 2008–2010. Finnish Meteorological Institute Reports 2014, 7.

Manninen, T., Rantasuo, M., Le Toan, T., Davidson, M., Mattia, F., & Borgeaud, M. (1998). Multiscale surface roughness of bare soil, in Proceedings of the IGARSS'98, pp. 1203–1206, IEEE International, Seattle, 6–10 July.

Markus, T., Stroeve, J. C., & Miller, J. (2009). Recent changes in Arctic sea ice melt onset, freezeup, and melt season length. *Journal of Geophysical Research, 114*, C12024, doi: 10.1029/2009JC005436.

Martini, A., Desieu, J.-P., Ferro-Famil, L., Bernier, M., & Pottier, E. (2006). Snow extent mapping in alpine areas using polarimetric SAR data. *EARSeL proceedings*, *5*, 129-136.

Mellor, M. (1965). Cold Regions Science and Engineering part III, Section A3c: Blowing Snow. Cold Regions Research and Engineering Laboratory, Hanover, USA.

Ménégoz, M., Krinner, G., Balkanski, Y., Cozic, A., Boucher, O., & Ciais, P. (2013). Boreal and temperate snow cover variations induced by black carbon emissions in the middle of the 21st century. *The Cryosphere*, *7*(2), 537-554.

Mialon, A., Fily, M., & Royer, A. (2005). Seasonal snow cover extent from microwave remote sensing data: comparison with existing ground and satellite based measurements. *EARSeL eProceeding*, *4*, 215–225 (http://www.eproceedings.org/static/vol04_2/04_2_mialon1.pdf).

Myers-Smith, I. H., Forbes, B. C., Wilmking, M., Hallinger, M., Lantz, T., Blok, D., ... & Boudreau, S. (2011). Shrub expansion in tundra ecosystems: dynamics, impacts and research priorities. *Environmental Research Letters*, *6*(4), 045509.

Nagler, T., & Rott, H. (2000). Retrieval of wet snow by means of multitemporal SAR data. *Transactions on Geoscience and Remote Sensing, 38*(2), 754-765.

Nakaya, U. (1954). *Snow crystal, natural and artificial*. Harvard University Press.

Pan, Y. D., Birdsey, R.A., Fang, J., Houghton, R., Kauppi, P.E., Kurz, W.A., Phillips, O.L., Shvidenko, A., Lewis, S.L., Canadell, J.G., Ciais, P., Jackson, R.B., Pacala, S.W., McGuire, A.D., Piao, S., Rautiainen, A., Sitch, S., & Hayes, D. (2011). A large and persistent carbon sink in the world's forests. *Science, 333*, 988-993.

Pearson, R. G., Phillips, S. J., Loranty, M. M., Beck, P. S., Damoulas, T., Knight, S. J., & Goetz, S. J. (2013). Shifts in Arctic vegetation and associated feedbacks under climate change. *Nature Climate Change*, *3*(7), 673.

Peltoniemi, J. I., Suomalainen, J., Hakala, T., Puttonen, E., Näränen, J., Kaasalainen, S., Torppa, J., & Hirschmugl, M. (2010). Reflectance of various snow types: measurements, modelling and potential for snow melt monitoring. In *Light Scattering Reviews 5: Single Light Scattering and Radiative Transfer*, chapter 9, 393-450. Springer Berlin Heidelberg. Doi: 10.1007/978-3-642-10336-0.

Petrovic, J. J. (2003). Review Mechanical properties of ice and snow. *Journal of Materials Science*, *38*, Issue 1, 1–6.

Piao, S., Wang, X., Ciais, P., Zhu, B., & Wang, T. (2011). Changes in satellite-derived vegetation growth trend in temperate and boreal Eurasia from 1982 to 2006. *Global Change Biology, 17,* 3228-3239.

Picard, G., Arnaud, L., Panel, J. M., & Morin, S. (2016). Design of a scanning laser meter for monitoring the spatio-temporal evolution of snow depth and its application in the Alps and in Antarctica. *The Cryosphere*, *10*, 1495-1511.

Pirazzini, R. (2004). Surface albedo measurements over Antarctic sites in summer. *Journal of Geophysical Research*, *109*(D20118).

Pirazzini, R., Räisänen, P., Vihma, T., Johansson, M., & Tastula, E. M. (2015). Measurements and modelling of snow particle size and shortwave infrared albedo over a melting Antarctic ice sheet. *The Cryosphere*, *9*(6), 2357-2381.

Prokop, A. (2008). Assessing the applicability of terrestrial laser scanning for spatial snow depth measurements. *Cold Regions Science and Technology*, *54*, 155–163.

Prokop, A., Schirmer, M., Rub, M., Lehning, M., & Stocker, M. (2008). A comparison of measurement methods: terrestrial laser scanning, tachymetry and snow probing for the determination of the spatial snow-depth distribution on slopes. *Annals of Glaciology*, *49*, 210–216.

Rees, W. G. (1998). A rapid method for measuring snow surface profiles. *Journal of Glaciology*, *44*(148), 674–675.

Rees, W. G., & Arnold, N. S. (2006). Scale-dependent roughness of a glacier surface: Implications for radar backscatter and aerodynamic roughness modelling. *Journal of Glaciology*, *52*, 214– 222.

Riggs, G. A., & Hall, D. K. (2015). MODIS Snow Products Collection 6 User Guide. https://nsidc.org/sites/nsidc.org/files/files/MODIS-snow-user-guide-C6.pdf

Rigina, O. (2002). Environmental impact assessment of the mining and concentration activities in the Kola Peninsula, Russia by multidate remote sensing. *Environmental monitoring and assessment, 75,* 11-31.

Rott, H. (1984). The analysis of backscattering properties from SAR data of mountain regions. *Journal of Oceanic Engineering*, OE-9(5), 347–355.

Roujean, J. L., Manninen, T., Kontu, A., Peltoniemi, J., Hautecoeur, O., Riihelä, A., ... & Sukuvaara, T. (2009, July). SNORTEX (Snow Reflectance Transition Experiment): Remote sensing measurement of the dynamic properties of the boreal snow-forest in support to climate and weather forecast: report of IOP-2008. In *Geoscience and Remote Sensing Symposium, 2009 IEEE International, IGARSS 2009* (Vol. 2, pp. II-859). IEEE.

Schaaf, C. B., Gao, F., Strahler, A. H., Lucht, W., Li, X., Tsang, T., ... & Lewis, P. (2002). First operational BRDF, albedo nadir reflectance products from MODIS. *Remote sensing of Environment*, *83*(1-2), 135-148.

Schaepman-Strub, G., Schaepman, M. E., Painter, T. H., Dangel, S., & Martonchik, J.V. (2006). Reflectance quantities in optical remote sensing – definitions and case studies. *Remote Sensing of Environment*, *103*, 27-42.

Schirmer, M., & Lehning, M. (2011). Persistence in intra-annual snow depth distribution: 2. Fractal analysis of snow depth development. *Water Resources Research*, *47*, W09517, 14 pp.

Scipión, D. E., Mott, R., Lehning, M., Schneebeli, M., & Berne, A. (2013). Seasonal small-scale spatial variability in alpine snowfall and snow accumulation. *Water Resources Research*, *49*, 1446-1457.

Shaker, A., Yan, W. Y., & El-Ashmawy, N. (2011). The effects of laser reflection angle on radiometric correction of the airborne lidar intensity data. *Int. Arch. Photogramm. Remote Sens. Spat. Inf. Sci.*, *38* (5/W12), 213-217.

Shi, J., & Dozier, J. (2000). Estimation of Snow Water Equivalence Using SIR-C/X-SAR, Part II: Inferring Snow Depth and Particle Size. *IEEE Transactions on Geosciences and Remote Sensing, 38*(6), 2475-2488.

Sicart, J. E., Ribstein, P. Wagnon, P., & Brunstein D. (2001). Clear-sky albedo measurements on a sloping glacier surface: A case study in the Bolivian Andes. *Journal of Geophysical Research*, *106* (D23), 31729–31737, doi:10.1029/2000JD000153.

Siljamo, N., & Hyvärinen, O. (2011). New Geostationary Satellite–Based Snow-Cover Algorithm. *Journal of Applied Meteorology and Climatology*, *50*(6), 1275-1290.

Smith, N., Saatchi, S., & Randerson, J. (2004). Trends in high northern latitude soil freeze and thaw cycles from 1988 to 2002. *Journal of Geophysical Research*, *109,* D12101, 14 p.

Sommerfeld, R. A., & LaChapelle, E. (1970). The classification of snow metamorphism. *Journal of Glaciology, 9*(55), 3-17.

Stocker, T. (Ed.). (2014). *Climate change 2013: the physical science basis: Working Group I contribution to the Fifth assessment report of the Intergovernmental Panel on Climate Change*. Cambridge University Press.

Sturm, M., Holmgren, J., & Liston, G. (1995). A Seasonal Snow Cover Classification System for Local to Global Applications. *Journal of Climate, 8,* 1261-1283.

Sturm, M., Racine, C., & Tape, K. (2001). Climate change: increasing shrub abundance in the Arctic. *Nature*, *411*(6837), 546.

Sturm, M., Douglas, T., Racine, C., & Liston, G. (2005). Changing snow and shrub conditions affect albedo with global implications. *Journal of Geophysical Research: Biogeosciences*, *110,* G01004, doi:10.1029/2005JG000013.

Tape, K. E. N., Sturm, M., & Racine, C. (2006). The evidence for shrub expansion in northern Alaska and the Pan-Arctic. *Global Change Biology*, *12*(4), 686-702.

Thackeray, C. W., Fletcher, C. G., & Derksen, C. (2015). Quantifying the skill of CMIP5 models in simulating seasonal albedo and snow cover evolution. *Journal of Geophysical Research: Atmospheres*, *120*(12), 5831-5849.

Trenberth, K.E. *et al*. In Solomon, S. (Ed.). (2007). *Climate change 2007-the physical science basis: Working group I contribution to the fourth assessment report of the IPCC* (Vol. 4). Cambridge University Press.

Trujillo, E., Ramírez, J. A., & Elder, K. (2007). Topographic, meteorological, and canopy controls on the scaling characteristics of the spatial distribution of snow depth fields, *Water Resources Research.*, *43*, W07409, doi: 10.1029/2006WR005317.

Ulaby, F. T., Moore, R. K., & Fung, A. K. (1982). Microwave Remote Sensing, vol. II, Addison-Wesley, Reading.

Van der Veen, C. J., Ahn, Y., Csatho, M., Mosley-Thompson, E., & Krabill, W. B. (2009). Surface roughness over the northern half of the Greenland Ice Sheet from airborne laser altimetry. *Journal of Geophysical Research*, *114*, F01001, doi:10.1029/2008 JF001067.

Várnai, T., & Cahalan, R. F. (2007). Potential for airborne offbeam lidar measurements of snow and sea ice thickness. *Journal of Geophysical Research: Oceans*, *112*(C12).

Veitinger, J., Sovilla, B., & Purves, R. S. (2014). Influence of snow depth distribution on surface roughness in alpine terrain: a multi-scale approach. *The Cryosphere*, *8*(2), 547.

Wagner, W., Ullrich, A., Ducic, V., Melzer, T., & Studnicka, N. (2006). Gaussian decomposition and calibration of a novel small footprint full-waveform digitizing airborne laser scanner. *ISPRS Journal of Photogrammetry and Remote Sensing*, *60*, 100-112.

Wang, L., Derksen, C., Brown, R., & Markus, T. (2013). Recent changesin pan-Arctic melt onset from satellite passive microwave measurements. *Geophysical Research Letters*, *40*, 1-7.

Warren, S. (1982). Optical properties of snow. *Reviews of Geophysics and space physics, 20*(1), 67-89.

Warren, S. (1984). Impurities in snow: effects on albedo and snowmelt (review). *Annals of Glaciology*, *5,* 177-179.

Warren, S. G., Brandt, R. E., & Grenfell, T. C. (2006). Visible and near-ultraviolet absorption spectrum of ice from transmission of solar radiation into snow. *Applied optics*, *45*(21), 5320-5334.

Warren, S., Brandt, R., & Hinton, P. (1998). Effect of surface roughness on bidirectional reflectance of Antarctic snow. *Journal of Geophysical Research, 103*(E11), 25789-25807.

Warren, S. G., & Wiscombe, W. J. (1980). A model for the spectral albedo of snow. II: Snow containing atmospheric aerosols. *Journal of the Atmospheric Sciences, 37*(12), 2734-2745.

Weiser, U., Olefs, M., Schöner, W., Weyss, G., & Hynek, B. (2016). Correction of broadband snow albedo measurements affected by unknown slope and sensor tilts. *The Cryosphere*, *10*, 775-790.

Weligepolage, K., Gieske, A. S. M., & Su, Z. (2012). Surface roughness analysis of a conifer forest canopy with airborne and terrestrial laser scanning techniques. *International journal of applied earth observation and geoinformation: JAG*, *14*, 192–203 (1).

Williams, L. D., & Gallagher, J. G. (1987). The Relation of Millimetre-Wavelength Backscatter to Surface Snow Properties. *IEEE Transactions on Geoscience and Remote Sensing*, *GE-25*(2), 188-193.

Williams, L. D., Gallagher, J. G., Sugden, D. E., & Birnie, R. V. (1988). Surface snow properties effects on millimeter-wave backscatter. *Transactions on Geoscience and Remote Sensing*, *26*(3), 300–306.

Winkler, R. D., Apittlehouse, D. L., & Golding, D. L. (2005). Measured differences in snow accumulation and melt among clearcut, juvenile and mature forests in southern British Columbia. *Hydrological Processes*, *19*, 51-62.

Wiscombe, W. J., & Warren, S. G. (1980). A Model for the Spectral Albedo of Snow, I: Pure Snow. *Journal of the Atmospheric Sciences*, *37*, 2712– 2733.

Woodhouse, I.H. (2006). Introduction to Microwave remote sensing, Taylor and Francis Group, Boca Ranton.

Xu, L., Myneni, R. B., Iii, F. C., Callaghan, T. V., Pinzon, J. E., Tucker, C. J., ... & Euskirchen, E. S. (2013). Temperature and vegetation seasonality diminishment over northern lands. *Nature Climate Change, 3*(6), 581-586.

Yan, W.Y., Shaker, A., Habib, A., & Kersting, A.P. (2012). Improving classification accuracy of airborne LiDAR intensity data by geometric calibration and radiometric correction. *ISPRS J. Photogramm. Remote Sens., 67*, 35-44.

Zhuravleva, T. B., & Kokhanovsky, A. A. (2011). Influence of surface roughness on the reflective properties of snow. *Journal of Quantitative Spectroscopy and Radiative Transfer, 112*, 1353–1368.